Organisation for Economic Co-operation and Development

ENV/CBC/MONO(2022)28

Unclassified

English - Or. English

1 September 2022

ENVIRONMENT DIRECTORATE
CHEMICALS AND BIOTECHNOLOGY COMMITTEE

Case Study on the use of Integrated Approaches for Testing and Assessment for developmental neurotoxicity hazard characterisation of imidacloprid and the metabolite desnitro-imidacloprid

Series on Testing and Assessment
No. 366

JT03501679

OECD Environment, Health and Safety Publications

SERIES ON TESTING AND ASSESSMENT

NO. 366

Case Study on the use of Integrated Approaches for Testing and Assessment for developmental neurotoxicity hazard characterisation of imidacloprid and the metabolite desnitro-imidacloprid

IOMC

INTER-ORGANIZATION PROGRAMME FOR THE SOUND MANAGEMENT OF CHEMICALS

A cooperative agreement among FAO, ILO, UNDP, UNEP, UNIDO, UNITAR, WHO, World Bank and OECD

Environment Directorate

ORGANISATION FOR ECONOMIC COOPERATION AND DEVELOPMENT

Paris 2022

About the OECD

The Organisation for Economic Co-operation and Development (OECD) is an intergovernmental organisation in which representatives of 38 industrialised countries in North and South America, Europe and the Asia and Pacific region, as well as the European Commission, meet to co-ordinate and harmonise policies, discuss issues of mutual concern, and work together to respond to international problems. Most of the OECD's work is carried out by more than 200 specialised committees and working groups composed of member country delegates. Observers from several countries with special status at the OECD, and from interested international organisations, attend many of the OECD's workshops and other meetings. Committees and working groups are served by the OECD Secretariat, located in Paris, France, which is organised into directorates and divisions.

The Environment, Health and Safety Division publishes free-of-charge documents in twelve different series: **Testing and Assessment**; **Good Laboratory Practice and Compliance Monitoring**; **Pesticides**; **Biocides**; **Risk Management**; **Harmonisation of Regulatory Oversight in Biotechnology**; **Safety of Novel Foods and Feeds; Chemical Accidents; Pollutant Release and Transfer Registers; Emission Scenario Documents; Safety of Manufactured Nanomaterials;** and **Adverse Outcome Pathways.** More information about the Environment, Health and Safety Programme and EHS publications is available on the OECD's World Wide Web site (www.oecd.org/chemicalsafety/).

This publication was developed in the IOMC context. The contents do not necessarily reflect the views or stated policies of individual IOMC Participating Organizations.

The Inter-Organisation Programme for the Sound Management of Chemicals (IOMC) was established in 1995 following recommendations made by the 1992 UN Conference on Environment and Development to strengthen co-operation and increase international co-ordination in the field of chemical safety. The Participating Organisations are FAO, ILO, UNDP, UNEP, UNIDO, UNITAR, WHO, World Bank and OECD. The purpose of the IOMC is to promote co-ordination of the policies and activities pursued by the Participating Organisations, jointly or separately, to achieve the sound management of chemicals in relation to human health and the environment.

This publication is available electronically, at no charge.

- **Also published in the Series on Testing and Assessment: link**

For this and many other Environment, Health and Safety publications, consult the OECD's World Wide Web site (www.oecd.org/chemicalsafety/)

or contact:

OECD Environment Directorate,
Environment, Health and Safety Division
2 rue André-Pascal
75775 Paris Cedex 16
France

E-mail: ehscont@oecd.org

Foreword

OECD member countries have been making efforts to expand the use of alternative methods in assessing chemicals. The OECD has been developing guidance documents and tools for the use of alternative methods such as (Q)SAR, chemical categories and Adverse Outcome Pathways (AOPs) as a part of Integrated Approaches for Testing and Assessment (IATA). There is a need for the investigation of the practical applicability of these methods/tools for different aspects of regulatory decision-making, and to build upon case studies and assessment experience across jurisdictions.

The objective of the IATA Case Studies Project is to increase experience with the use of IATA by developing case studies, which constitute examples of predictions that are fit for regulatory use. The aim is to create common understanding of using novel methodologies and the generation of considerations/guidance stemming from these case studies. This case study was developed for illustrating practical use of IATA and submitted to the 2021 review cycle of the IATA Case Studies Project.

The case study was reviewed by the project team, and endorsed at the 6th meeting of the Working Party on Hazard Assessment in June 2022.

The case study is illustrative examples, and their publication as OECD monographs does not translate into direct acceptance of the methodologies for regulatory purposes across OECD countries. In addition, the cases study should not be interpreted as official regulatory decisions made by the authoring member countries.

This document is published under the responsibility of the Chemicals and Biotechnology Committee of the OECD.

Acknowledgements

The authors of this Case Study were

Jonathan Blum [2)]*, Ylva Johansson[1)]*, Rebecca von Hellfeld[3)] , Thomas Braunbeck[3)], María Hinojosa[1)], Melinda Zana [4)], Andras Dinnyes [4)], Dominik Loser[2)8)], Marcel Leist [2)], Karin Grillberger [5)], Gerhard Ecker[5)], Barbara M.A. van Vugt-Lussenburg[6)], Bart van der Burg[6)], Iain Gardner[7)], Anna Forsby[1)]¤, Susanne Hougaard Bennekou[10)]¤.

*Contributed equally

¤Corresponding authors

Affiliation at time of contribution:

1) Department of Biochemistry and Biophysics, Stockholm University, Stokholm Sweden

2) In Vitro Toxicology and Biomedicine, Department Inaugurated by the Doerenkamp-Zbinden Foundation, University of Konstanz, Universitaetsstr. 10, 78457, Konstanz, Germany

3) University of Heidelberg, Centre of Organismal Studies, Im Neuenheimer Feld 504, 69120 Heidelberg, Germany

4) BioTalentum Ltd., H-2100 Gödöllő, Hungary

5) Department of Pharmaceutical Sciences, University of Vienna, Vienna, Austria

6) BioDetection Systems bv Science Park 406, 1098XH Amsterdam, The Netherlands

7) CERTARA UK Limited, Simcyp Division, Level 2-Acero, 1 Concourse Way, Sheffield, S1 2BJ, UK

8) NMI Natural and Medical Sciences Institute at the University of Tübingen, 72770, Reutlingen, Germany

9) University of Aberdeen, 23 St Machar Drive, Old Aberdeen, AB24 3UU

10) Technical University of Denmark, Kongens Lyngby, Denmark

Table of contents

FIGURES

TABLES

List of abbreviations

AChBP	Acetylcholine binding protein
ADHD	Attention deficit hyperactivity disorder
AO	Adverse outcome
AOP	Adverse outcome pathway
BDNF	Brain derived neurotrophic factor
BIOT	BioTalentum Ltd
DEG	Differentially expressed gene
DNT	Developmental neurotoxicity
EC	Effect concentration
FET	Fish embryo acute toxicity
hiPSC	human induced pluripotent stem cell
hpf	hours post fertilization
IVB	*In vitro* battery
KE	Key event
LOEC	Lowest effect concentration
LOQ	Limit of quantitation
LUHMES	Lund human mesencephalic
MIE	Molecular initiating event
nAChR	Nicotinic acetylcholine receptor
NAM	New approach method
NCCs	Neural crest cells
NEP	Neuroepithelial precursor
NOAEL	No-observed-adverse-effect-level
OECD	Organization for Economic Co-operation and Development
PBTK	Physiologically based toxicokinetic
PRISMA:	Preferred Reporting Items for Systematic Reviews and Meta-Analyses
PND	Postnatal day
VOCC	Voltage-operated-calcium-channels

Executive Summary

The EFSA Scientific Opinion on the developmental neurotoxicity potential of acetamiprid and imidacloprid (2013) concluded that there were uncertainties that prevented a firm conclusion on neuropathological findings in females in the caudate-putamen at the highest tested dose of 54,5 mg/kg bw /day in an OECD TG426 regulatory study on imidacloprid. The mechanistic data by Kimura-Kuroda (2012) did provide some mechanistic understanding but the study had limitations. Deriving from the uncertainties elaborated in this opinion, the hypothesis for this IATA is that mechanistic understanding of the toxicodynamic properties of imidacloprid contextualized with internal exposure considerations from realistic human exposures can inform the hazard characterization regarding potential DNT effect.

In this case study, further evidence has been collected, appraised, and assessed by updating a review performed by Sheets *et al* (2016). *In vivo* data shows that imidacloprid could result in alterations in learning and behavior. One study provided evidence of altered behavior in offspring of female mice treated with a low dose of 0.5 mg/kg/bw imidacloprid per day. *In vitro* data available shows that imidacloprid exposure induces Ca^{2+} via the nAChRs as well as attenuated voltage-operated-calcium-channels (VOCC) function. In addition, several *in vitro* studies have investigated morphological and transcriptional changes due to imidacloprid exposure, but no uniform effects have been observed. In addition, there is evidence that the desnitro-imidacloprid metabolite formed in mammals and in the environment, including crops sprayed with imidacloprid and is thought to have a higher potency to act on mammalian receptors than its parent compound.

Thus, further *in vitro* and *in silico* data has been generated, characterizing the effects of imidacloprid and desnitro-imidacloprid in a battery of DNT *in vitro* test anchored to a postulated AOP as well as additional screening for nuclear receptor activation. In addition, the *in vitro* toxicodynamic data has been contextualized with internal exposure predictions by PBPK modelling. Although, the MIE and early KEs of the proposed AOP have in this report been firmly established, significant uncertainties remain both related to an adverse outcome and key events adjacent to the adverse outcome.

1 Introduction

1.1 Background

The human brain develops through a series of developmental stages that must occur in a particular sequence and at the right time. The outcome on the human brain is critically dependent upon the physiology of these processes, each of which might be vulnerable to adverse effects from exposures to environmental chemicals or drugs.

Study guideline for rodent developmental neurotoxicity (DNT) has been available for a considerable time (US Environmental Protection Agency (OPPTS 870.630), The Organization for Economic Co-operation and Development (OECD, 2007[1]; OECD, 2018[2]; USEPA, 1998[3]), including guidance for interpreting DNT data (North American Free Trade Agreement (NAFTA) Technical Working Group on Pesticides (TWG), 2017[4]). However, DNT testing is not carried out routinely under any chemical's regulation. DNT testing is only triggered when neurotoxic or endocrine effects is observed in adult rodents. These triggers may not be sufficient (Bal-Price *et al*., 2018[5]) as some neurodevelopmental processes are not present in the adult brain (Fritsche *et al*., 2017[6]). Performance of the DNT *in vivo* guideline studies involves the use of large numbers of animals and is therefore cost- and time-intensive (Crofton *et al*., 2012[7]), they are difficult to interpret, together with the considerable uncertainties related to *in vivo* DNT models (Paparella *et al.,* 2020[8]). All together this has fostered efforts to develop *in vitro* methods that combined in an DNT *in vitro* battery (IVB) reflects the main processes behind the development of the nervous system that can lead to adverse effects (Bal-Price *et al*., 2018[5]; Masjosthusmann *et al*.,2020[9]) To support regulatory use of an IVB, the OECD has taken up the activity of developing a guidance for interpretation of data generated from an IVB in the context of an IATA.

1.2 Problem Formulation

This case study aims to develop an IATA that could support hazard identification/characterization based on a problem formulation originating from the EFSA Scientific Opinion on developmental neurotoxicity potential of two neonicotinoid pesticides one being imidacloprid (EFSA, 2013[10]). The scientific opinion was initiated based on *in vitro* data indicating that imidacloprid induced excitation and/or desensitization of nicotinic acetylcholine receptors (nAChRs) in rat neonatal cerebellar neurons and the authors concluded that imidacloprid might have affect the developing brain similarly to nicotine (Kimura-Kuroda *et al.*, 2012[11]).

The scientific opinion outlined the uncertainties for use of some *in vitro* data in the risk assessment of two neonicotinoid pesticides. The uncertainties included:

- the very limited biological 'space' covered by the assay (i.e., only nACh receptors),
- the need for further characterization of the assay in terms of relevance to *in vivo* end points,
- the need for data from positive and negative controls, and
- an assessment of the reliability and reproducibility of the assay.

The scientific opinion concluded that these uncertainties "prevent its current use as a screening tool in the regulatory arena".

On the other hand, the available DNT study on imidacloprid did not allow a full characterization of developmental neurotoxicity (EFSA, 2013[10]). Overall, there was residual uncertainty regarding establishing human reference dose (acute) which was mitigated by proposing additional safety factors.

The imidacloprid metabolite, desnitro-imidacloprid can be formed in mammals, in the environment including on crops. The desnitro-IMI is more active on mammalian α4β2 receptors than the corresponding insect systems and more toxic to mammals than the parent insecticide. This metabolite shows high affinity to and/or agonist potency at the mammalian α4β2 nAChR subtype comparable to that of nicotine (Tomizawa and Casida, 2003[12]).

Hence, in this case study, the problem formulation is derived from these uncertainties and is: Can NAM data in an IATA context (integrating existing information) on imidacloprid and its metabolite, desnitro-imidacloprid, sufficiently characterize DNT hazard?

1.3 Purpose

This IATA case study was developed to provide an example of the use and application of the DNT-IVB for a single substance DNT hazard assessment.

Furthermore, the case study also aims to address the uncertainties identified in EFSA 2013[10] in some of the *in vitro* and *in vivo* data to demonstrate that NAM data in an IATA context (integrating existing information) on acetamiprid. This is pursued by further DNT hazard characterisation and a contextualisation to exposure and risk by the use of PBK modelling.

The data derive from a case study on neonicotinoid pesticides conducted by the H2020-funded project "EU-ToxRisk". Here acetamiprid, imidacloprid, thiacloprid, thiamethoxam, dinotefuran, clothianidin and nicotine were tested in a range of *in vitro* assays, also assays as such not part of the current "OECD IVB". Testing and results on the other neonicotinoid compounds can be found in Loser *et al*. 2021a[13] and Loser *et al*. 2021b[14] and are not further discussed in the present case.

1.4 Chemical

The target chemical for this case study was the pesticide imidacloprid (CAS number 138261-41-3) and one of its metabolites, desnitro-imidacloprid (CAS number 115970-17-7). The chemical structure is shown in Figure 1.

Figure 1. The chemical structure of imidacloprid (left) and desnitro-imidacloprid (right).

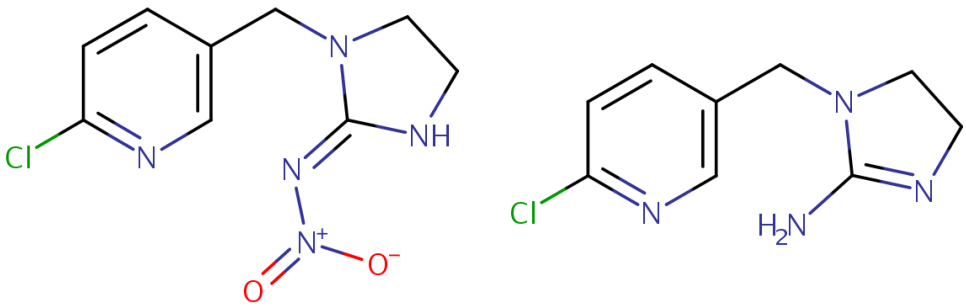

Imidacloprid is a neonicotinoid insecticide that triggers nervous system disturbances by activation of the nicotinic acetylcholine (ACh) receptor (nAChR) (Brown *et al*., 2006[15]; Tan *et al*., 2007[16]). The compounds are widely used in agriculture for pest control, although recently the use in Europe has been very restricted due to toxicity to pollinators. Neonicotinoids have been designed to display a high species specificity showing a high potency on insect receptors, while having low affinities on mammalian receptors (Casida, 2018[17]). Based on regulatory studies, imidacloprid has been classified according to CLP (EC 1272/2008) as harmful if swallowed (LD50 approx. 500 mg/kg bw). The critical effects were effects on body weight gain, liver effects in rats with NOAELs of 14 and 5,7 mg/kg in a 90-day and 2-year chronic toxicity studies, respectively. Neurotoxicity was also observed in an acute and a repeat-dose neurotoxicity study with NOAELs of 42 mg/kg bw and 9.3 mg/kg bw per day, respectively (EFSA, 2013[10]). Regarding the metabolite desnitro-imidacloprid, there are no mammalian toxicity data available, however the metabolite has similar specificity to vertebrate α4β2, α1 and α3 nAchR s as nicotine (EFSA, 2013[10]).

1.5 Endpoint

The endpoint of interest was DNT induced by exposure to imidacloprid being any adverse effect on the normal development of nervous system structure and/or function, as defined by different specific endpoints measured *in vivo*, *in vitro* and in human observational studies, for example startle response in TG426 protocols, calcium signaling in developing neuronal cells or learning and memory in human observational studies, respectively.

1.6 Exposure Information

Exposure considerations are integrated in this IATA. Dietary and non-dietary exposure to imidacloprid and desnitro-imidacloprid can occur by its use as a pesticide active substance. The case considers dietary exposure information obtained from the European monitoring program to pesticide residues in 2018 (EFSA, 2020[18]).

2 Hypothesis for performing the IATA

The hypothesis is that mechanistic understanding of the toxicodynamic properties of imidacloprid and its metabolite desnitro-imidacloprid contextualized with internal exposure considerations related to realistic human exposures can inform the hazard characterization in regard to potential DNT effect.

2.1 Rationale for the IATA and method

As outlined above, identified uncertainties both regarding the *in vitro* mechanistic data by Kimura-Kuroda *et al*., 2012[11] and the uncertainties identified from the regulatory TG426 study as analyzed by ESFA in 2013[10], led to the hypothesis, that further mechanistic understanding could reduce the uncertainty on the potential DNT hazard properties of imidacloprid. Mechanistic understanding provided by *in vitro* evidence is expected to contribute to the Weight of Evidence for the DNT hazard characterization. The IATA workflow contained the following steps.

1) Assembling of evidence (*in vitro*, *in vivo*, and human observational studies) updating a systematic literature review performed by Sheets *et al*. 2016[19].
2) Screening for relevance.
3) Integration of the evidence by an AOP-based approach.
4) Generation of additional mechanistic evidence and contextualization.
5) Data gap and uncertainty analysis.
6) Conclusion.

Only *in vivo* and *in vitro* studies from the literature assessed as relevance in terms of the identity of the tested substance, the model used, the endpoint studies and timing of exposure (during development). There was no relevant human observational data. No documented AOP exists for 'Binding to nAChR leading to behavioral effects' and thus a putative AOP was postulated. In the following step the results of testing of imidacloprid in the EU-ToxRisk testing systems were included as mechanistic evidence and were mapped into AOP endpoints network in addition to the evidence retrieved from the systematic literature review.

3 Data gathering and application of the IATA

Sheets *et al.* 2016 conducted a systematic review on neonicotinoid pesticides in regard to their DNT properties. For this case study, the review has been updated by applying the same search string and search in toxline form the date of the Sheets review (15.6.2015).

3.1 Summary of systematic review performed by Sheets *et al*. 2016[19]

Sheets *et al.* reviewed in total 5 *in vivo* studies and one *in vitro* study to collect existing evidence of neonicotinoid pesticides for DNT until mid 2015 (Table 1) (Sheets *et al*. 2016[19]).

Table 1. Reviewed literature by Sheets *et al.* 2016, table adapted from Sheets[19]

		Abou-Donia et al. (2008)	Tanaka (2012a)	Tanaka (2012b)	Ozdemir et al. (2014)	Crosby et al. (2015)
In vivo studies	English; full article with data tables	Yes	Yes	Yes	Yes	Yes
	"Single chemical: Not a mixture or formulation"	Yes	Yes	Yes	Yes	Yes
	"Chemical conc. and dose levels reported"	Yes	Yes	Yes	No/Yes	Yes
	"Explicit duration of exposure"	Yes	Yes	Yes	Yes	Yes
	"Distinguish DNT from acute neurotoxic effect"	Yes	Yes (GD0 - LD21)	No (repro study)	No (PND 7 to term)	Yes
	"Appropriate concurrent control for reference"	Yes	Yes	Yes	Yes	Yes
	"Test organism and sample size defined"	Yes	Yes	Yes	Yes	Yes
	"Relevant to human risk for DNT"	Yes	Yes	Yes	Yes	Unknown
In vitro studies		Kimura-Kuroda et al. (2012)				
	"English; full article with data tables"	Yes				
	"Findings relevant to DNT outcomes"	Yes				

Among these 5 *in vivo* studies only one was dealing with imidacloprid. Abou-Donia *et al.* 2008 performed a study with imidacloprid in pregnant Sprague-Dawley rats and found some evidence of neurobehavioral effects and GFAP expression changes in brain regions (Abou-Donia *et al.,* 2008[20]). However, the study has several limitations. I) Animals were treated with only a single dose. II) Single dose used was very high with 337 mg/bw imidacloprid, which corresponds to 75% of the acute oral LD50 in rats. III) The compound was administered intraperitoneal, which is an exposure route unlikely to be relevant for humans. These drawbacks in study design led to a conclusion by the authors themselves and the review study team of Sheets et. al that further research and investigations are needed to confirm the findings (Sheets *et al*., 2016[19] ;Abou-Donia *et al.* 2008[20]).

One *in vitro* study was reviewed (Kimura-Kuroda 2012). This study found, that in 14 day cultured primary cerebellar granule cells from rat, an excitatory Ca^{2+} influx can be measured with nicotine and imidacloprid. The findings in this study raised also an alert in the European food safety authority (EFSA) in 2013, as the high affinity to mammalian receptors by imidacloprid as found in this study are of high concern (EFSA, 2013[10]). The authors showed that the cellular system expresses relevant nAChR subunits. Still, there are

limitations of the study, concluded by Sheets *et al.* and the EFSA panel. That includes, that the effects on α7 and α4ß2 receptors could not be discriminated very clearly using inhibitors. As a positive control for nAChR stimuli, acetylcholine itself was not tested in the study. As a consequence, the mode of action leading to an influx in Ca^{2+} has to be investigated in more detail to decrease the uncertainty of this finding.

The OECD TG426 study both reviewed in EFSA and 2013 and by Sheets et al. (2016) both concluded that there were uncertainties that prevented a firm conclusion regarding the neuropathological findings in females in the caudate-putamen at the highest tested dose of 54,5 mg/kg bw /day, since its measures were not made at the lower doses.

In summary, this study review came to the conclusion that the given evidence is still limited. This is consistent with findings by the EFSA in 2013[10]. Especially, mechanistic understanding is still lacking and no further studies in this direction could decrease the uncertainty raised by the EFSA in 2013.

3.2 Summary of literature review performed in this study

To fill the gap of studies and evidence between the Sheets review in 2016 and the current study, a literature collection using the same criteria was performed. The publications were reviewed. This resulted in a total of 10 publications summarized below in Table 2.

Table 2. Summary of publications identified and reviewed after application of search string

Study design	Endpoints studied	Method	Cyto-toxicity /maternal toxicity	Effects /concentrations	Nicotine used as positive control	Source
Wister albino rats: a) newborn infants and b) adults	1. Learning activities 2. Gene expression levels / Transcriptomics	1. Morris water maze 2. qPCR of 4 genes. Brain tissues of animals.	Not determined	Overall doses tested: 0.5, 2, 8 mg/kg dose (given by gavage). Repeated dose (daily for 3 months). Solvent control included 1. Learning deficits at a) 2 and 8 mg/kg in pups b) 8 mg/kg in adults 2. GRIN1, SYP, GAP-43 altered, but not significantly M1 significantly changed at 8 mg/kg in adults	No	Kara et al., 2015[21]
Chick embryos	Imi effect on neurogenesis, focusing on neural tube defects (NTDs) at an early and late stage Early exposure - from HH0 to HH10 Late exposure - from HH10 during 4.5 days *in vivo* through injection	Immunohistochemistry In situ hybridisation Western blot RT-qPCR followed by protein protein interaction analysis TUNEL assay	Mortality measured.	HH10 chich embryos exposed to 62.5, 125, 250 and 500 µM Increased NDTs with increased concentration F-actin attenuation at 500 µM --> neural plate bending failure Late exposure led to neural tube re-open Alter gene expression at 500 µM at both early (Cx43, BMP4, Gli1, caspase9) and late (Pax6, Neurogenin2, Cyclin D1, p21) stage of development Supressed cell proliferation and apoptosis at 500 µM	No	Liu et al., 2016[22]
CD-1 mice. Male, female and offspring	1. Behavior – suitable tests selected based on nicotine	1. a) Open field test 1. b) Elevated plus maze 1. c) Forced swim test 1. d) Tube test 1. e) Resident	Not determined. Fecundity checked and	General dosing scheme: 0.5 mg/kg per day from gestational day 4 to end of lactation at postnatal day 21 Offspring from treated mothers showed 1. Behavior: i) Elevated motor activity ii) enhanced social dominance iii) reduced depressive behavior iv) diminution in social	Not directly Tests selected based on nicotine And 300	Burke et al., 2018[23]

	2. Serum biochemistry 3. Compound distribution in tissues 4. nAChR localisation	intruder test 2. Whole blood serum measure 3. LC/MS measures for quantification 4. Autoradiography with [³H]epitabidine	reduced with Imi.	aggression 2. Serum: Lower triglycerides 3. Imi in brain and livers of mothers. Only traces in some offspring 4. Significant difference in interpeduncular nucleus	µM Nicotine as blank in binding exp. But no Nicotine data shown in this publication	
Arc-promoter-driven luciferase transgenic mice strains. **Juvenile (4W), young adult (8W) and adults (3-6M) used**	1. Arc gene induction	1. Bioluminescence measurements of Arc in forebrain	Not determined	Dose scheme: Acute administration. i.p. inject. 40 mg/kg **No effects** observed with Imi compared to other pesticides or positive Ctrl kainic acid	No	Izumi et al., 2019[24]
DIV2 neonatal rat cerebellar neurons **14 days exposure (half of the medium was renewed every 2 days)**	1. Transcriptomics 2. Morphology	1. Whole genome microarray and RT-qPCR 2. Immunocytochemistry	By morphology (2)	One concentration tested (1 µM) 1. 4862 DEGs of 22852 genes in total Out of 67 selected DEGs: 27 up, 40 down. Down-regulation of Chrna7. Common genes in GO and DP: Cacna1h, Cacng1, Hrh2, F2rl2 2. No cytotoxicity, reduced dendritic area of purkinje cells	Yes, 1 µM	Kimura-Kuroda et al., 2016[25]
Neonatal mice	1. Neurogenesis in hippocampal dentate gyrus (DG) 2. Microglial activation in hippocampal DG	1. and 2. via immunohistochemistry	Not determined.	Dose scheme: 5 mg/kg/day (Positive Ctrl Nic 0.5 mg/kg/day) from postnatal day 12 to 26 by oral gavage 1. Reduction in neurogenesis 2 Increase in number of amoeboid-type and activated M1-type microglia	Yes	Nakayama et al., 2019[26]
Chick embryos and primary neuronal crest cells (NCC)	1. Craniofacial osteogenesis 2. NCC proliferation and apoptosis 3. Transcriptomics	1. Alizarin red staining 2. Immunofluorescent staining 3. In situ Hybridization and RT-qPCR	Survival and mortality rate determined	One concentration tested (500 µM) 1. Craniofacial osteogenesis and gastrulation development inhibited 2. NCC proliferation and apoptosis attenuated (48h exposure). Fewer NCCs in neural tube explants after 48h of exposure. 3 AChE1a, AChR downregulated after 12 days of exposure. Msx1, Sox9 FoxD3, BMP4, N-cadherin downregulated.	No	Wang et al., 2016[27]
Primary mouse neural stem/progenitor (NSPC) cells and mouse neuroblastoma-derived Neuro-2a cells (N2a)	1.Cytotoxicity 2. Metabolomics (performed only on NSPCs)	1. MTT assay (N2a) and tryptan blue staining (NSPC) 2. GC/EI/MS	Yes	1. Differentiated and undifferentiated N2a exposed to IMI (0-4000 µM) for 48 hours. $IC50_{diff}$ and $IC50_{undiff}$ > 4000 µM. NSPCs exposed to IMI (500, 700 and 900 µM) for 48 hours. IC50 = 710 µM. 2. NSPCs exposed to 710 µM IMI for 48 hours affected the metabolism. Increased glucose and lactate levels. Decreased levels of Kreb cycle intermediates fumarate, malate and succinate.	No, diazinon was used as a positive control	Fotopoulou et al., 2020[28]
PC12 cells (rat):NGF-induced differentiation, 5 days (medium renewed every 48 h)	1. Neurite outgrowth (NO) 2. Transcriptomics	1. Imaging, neurite length (ImageJ) 2. qPCR of 6 target genes	Not determined	1. No sign. altered NO at 1, 10, 100 µM. Weak, but not sign. at 100 µM 2. Down reg. at 100 µM: camk2a,	No	Christen et al., 2017[29]
Zebrafish embryo	1. Observe early	1.		1. In STC test:	Yes	Ogungbe

(ZFE)	behavioral changes in ZFE	Spontaneous tail coiling – STC (24-25 hpf)		Nicotine had "subtle effects considered to be conditional" IMI: no effect		mi et al., 2020[30]

In vivo

In a repeated dose toxicity test, Kara *et al* found significant effects in rats treated with imidacloprid (Kara *et al*., 2015[21]). In detail, using Morris water maze as a test method, they observed learning deficits in pups treated with 2 and 8 mg/kg/bw. A limitation of this study is that no positive reference chemical like nicotine was investigated.

Three studies investigated the effect of imidacloprid in mice. One study found that 5 mg/kg/day of imidacloprid in neonatal mice reduced neurogenesis in a hippocampal region (Nakayama *et al*., 2019[26]). A very extensive study in mice showed that imidacloprid treatments of 0.5 mg/kg/bw per day lead to significant behavioral changes in the offspring of female mice (Burke *et al*., 2018[23]). Several recognized tests were conducted (open field test, elevated plus maze, forced swim test, tube test, resident intruder test) and differences were found in i) elevated motor activity ii) enhanced social dominance iii) reduced depressive behavior iv) diminution in social aggression.

In vitro

One study investigated the potential of imidacloprid to alter the transcriptomic profile of cells *in vitro* (Kimura-Kuroda *et al.,* 2016[25]). For this, neonatal rat cerebellum cells were treated for 14 days with 1 µM of imidacloprid or nicotine. 67 differentially expressed genes in cells treated with imidacloprid were identified. An overlap of 5 genes relevant for neurodevelopment were found to be altered in cells treated with imidacloprid and nicotine. Similar to their previous study analyzing Ca^{2+} influx (Kimura-Kuroda *et al.,* 2012[11]), an uncertainty of this study is that the comparison of the effects of nicotine and imidacloprid raise questions. Even though nicotine should have a higher potency in mammalian cells acting via the nAChRs, nicotine altered less genes than imidacloprid (34 and 67 respectively). As a common mode of action for imidacloprid and nicotine is expected, it is also surprising that the number of overlapping genes is very low (5 genes). A general limitation of the study is that only a single concentration was tested and that a long treatment time (14 days) increases uncertainty to measure artefacts in transcriptomic changes. A study in P12 rat cells investigated the neurite outgrowth of the cells and found no significant alterations up to 100 µM (Christen *et al.,* 2017[29]). Two studies were performed in chicken embryos examining effects on cranial neural crest cells and neural tube formation (Liu *et al.*, 2016[22]; Wang *et al*.,2016[27]). However, concentrations leading to effects in these studies are of uncertain relevance for human exposure (500 µM). Both studies did not use nicotine as a positive control. Similar limitations (unrealistic high concentrations, no nicotine tested) lead to a high uncertainty in a study in NSPC and N2a cells (Fotopoulou *et al.,* 2020[28]).

ZFE

A study in zebrafish embryo (ZFE) examined the effect if imidacloprid on spontaneous tail coiling (STC) as an indicator of early behavioral changes in ZFE (Ogungbemi et al., 202030). They observed minor effects with nicotine as a positive control but did not notice any effect with ZFE treated with imidacloprid.

This systematic literature review added further studies to the previous studies examined by Sheets *et al*. in 2016. Behavioral effects found in three *in vivo* studies could give indications for a late adverse outcome event of imidacloprid. Especially the study by Burke *et al*., 2018 applied a broad panel of recognized tests to assess adverse behavioral outcomes (Burke *et al*., 2018[23]). Nevertheless, uncertainties remain. Mostly due to I) only single concentration testing II) Species differences and extrapolation of findings to humans III) often lack of positive reference chemicals such as nicotine. A study with high uncertainty gave

indications for gene transcription changes upon imidacloprid treatment *in vitro*. Other *in vitro* studies performed after 2016 could not provide clear further mechanistic understandings.

Based on this, we conducted this study using NAMs to decrease the remaining uncertainty from the available literature. In contrast to all pre-existing DNT *in vitro* literature of imidacloprid, we performed testing in mainly human cell-based test systems. As the findings of Kimura-Kuroda *et al*. 2012 remain one of the main concerns, but with a high uncertainty level, one main focus was to confirm these results in this study (Kimura-Kuroda *et al*. 2012[11]).

4 Absorption, distribution, metabolism, and excretion

Imidacloprid is a neutral compound with a reported Log P_{ow} of 0.57 (Pubchem). There have been relatively few studies that have studied the *in vivo* pharmacokinetics of imidacloprid although data for total radioactivity following dosing of ^{14}C-imidacloprid are available. Following dosing of 20mg/kg imidacloprid in corn oil to female rats the oral blood clearance of imidacloprid was 3.4 ml/min/kg (Kapoor *et al*. 2014[31]). Based on the reported AUC in blood and brain the tissue:blood ratio in female rats was calculated to be 0.47. In mice the brain:plasma ratio has been reported to be ~ 0.75 (Ford and Casida, 2006[32]).

In vivo in the rat imidacloprid is extensively metabolized. In the literature metabolism of imidacloprid by both aldehyde oxidase and cytochromes P450 have been reported (Ford and Casida, 2006[32]; Dick *et al*., 2005[33]; Kolanczyk *et al*., 2020[34] Schulz-Jander and Casida, 2002[35]; Schulz-Jander *et al*., 2002[36]; Wang *et al*., 2018[37]). The different routes of metabolism of imidacloprid have been summarized in the review by Wang *et al*.(2018)[37]. CYP isozymes including CYP3A4, 2C19,2A6 and2C9 were shown to form 5-hydroxy imidacloprid and lower amounts of the olefin and desnitro metabolite (Schulz-Jander and Casida, 2002[35] ;Schulz-Jander *et al*., 2002[36]). Other reports show the formation of more potent metabolites of imidacloprid by aldehyde oxidase with little increase in potency was seen when imidacloprid was incubated with CYP 3A4 (Honda *et al*.,2006[38]). Other studies have shown that aldehyde oxidase reduces imidacloprid but detected an aminoguanidine product rather than a guanidine (desnitro) metabolite (Dick *et al*., 2005[33]).

In the *in vitro* metabolism studies conducted in human hepatocytes for the EU_TOX-Risk project although metabolism of parent imidacloprid was too slow to accurately quantify the disappearance of imidacloprid (see below for further information) and calculate an *in vitro* intrinsic clearance, formation of some metabolites of imidacloprid were observed in human hepatocytes. However, the only metabolites observed were the 5-OH and olefin metabolites which are thought to be formed by CYP isozymes. This is despite the cells showing the capability to metabolize known aldehyde oxidase substrates such as carbazeran (Dalviea and Di, 2019[39]). Further studies to characterize the metabolism of imidacloprid with the aim of being able to determine the rate and extent of the metabolism of imidacloprid to the desnitro metabolite are ongoing.

5 MoA; nicotinic acetylcholine receptors (nAChR)

nAChR are ligand gated cation channels. The receptors are assembled of 5 subunits which can form heteromeres or homomeres with ligand-binding extracellular and ion channel transmembrane domains. The most abundant isoforms in brain are the heteropentameric α4β2nAChR and the homopentameric α7nAChR (Wada *et al.*, 1989[40]; Tribollet *et al.*, 2004[41]). The α4β2nAChR is more permeable for Na+ ions than for Ca^{2+} but the α7nAChR is more permeable for Ca^{2+} (Buisson *et al.*, 1996[42]; Seguela *et al.*, 1993[43]. This receptor is also rapidly desensitized upon ligand binding, and it is debated if receptor activation and Ca^{2+} influx is mediating the desensitization or if the receptor inactivation can take place by a conformational change upon ligand binding, i.e., an allosteric modulation (Williams *et al.*, 2011[44]).

Figure 2. 5.1 Pentameric structure of nAChR;
A) top view of heteropentameric α4β2 (with stoichiometry 3*α4 (blue protein ribbon) and 2*β2 (grey ribbon): PDB-ID 6cnk) (Walsh *et al*., 2018[45]);
B) side view of 2 adjacent full-length subunits that are forming the ligand (e.g. nicotine – green calotte model) binding site;
C) ECD of homopentameric α7 (ribbon in yellow – binding site residues in stick representation and circled: homology model (Ng *et al*.,2018[46])).

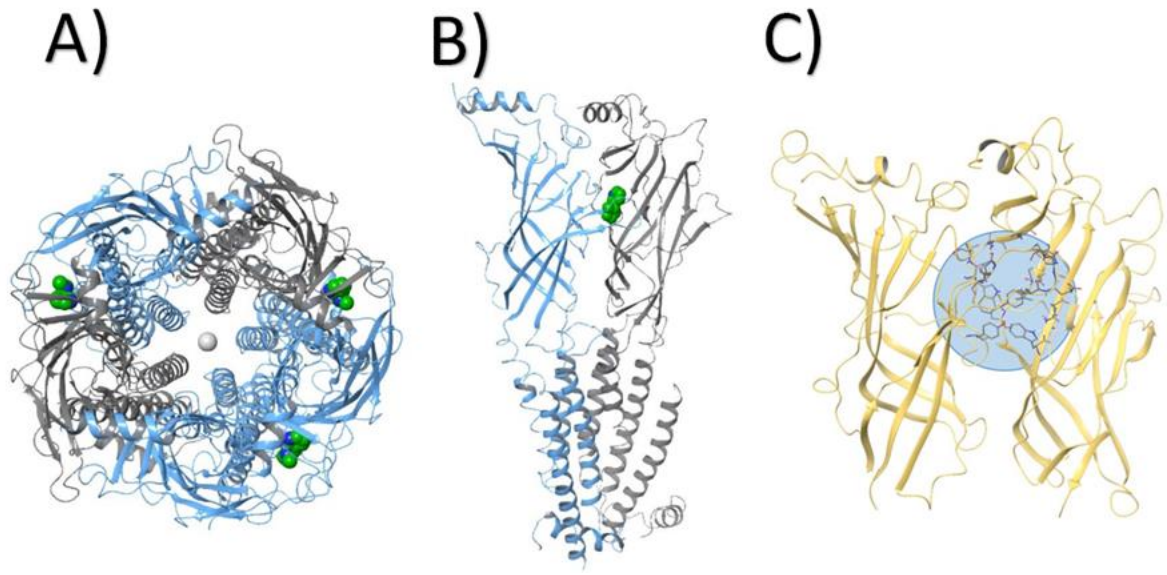

Neurodevelopment is orchestrated by cues such as neurotransmitters, growth and neurotrophic factors giving signals to the cell to take actions in a precise timely manner (Figure 3). Hence, altered signaling at specific sensitive windows during neurodevelopment could have an impact on proliferation, apoptosis, migration, differentiation, and synaptogenesis, i.e., cellular organization and maturation that will have an impact on brain function.

Figure 3. Schematic representation of how neurotransmitter signals control neuronal cell development during specified critical periods.

Depending on the context in which stimulation occurs, the same neurotransmitter, operating through the same receptors and signaling pathways, can promote cell replication, can elicit a switch from replication to differentiation, can promote or arrest cell growth, can evoke apoptosis, or can program the genes that determine the future responsiveness of the cell to external stimulation (cell learning). Figure from Slotkin *et al*., 2008[47].

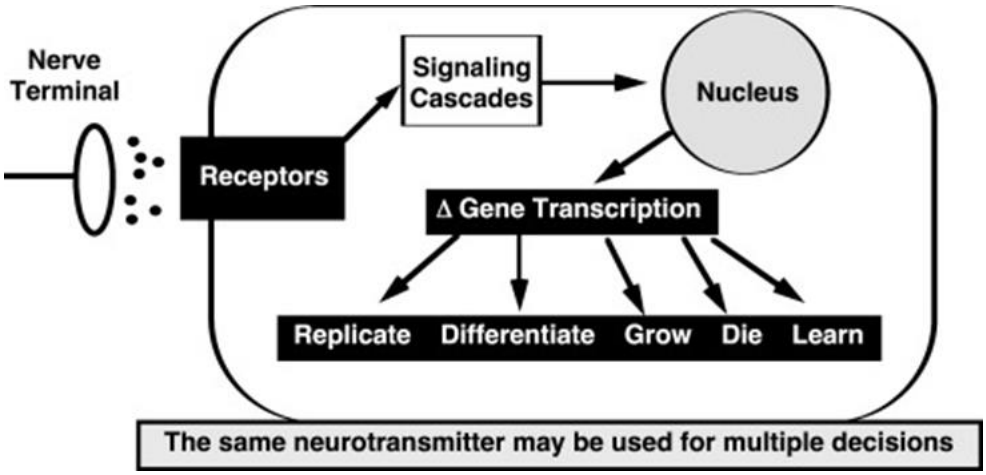

The nAChRs play central roles during neurodevelopment and the transient patterns in nAChR subtype expression during embryogenesis have different impact on each developmental stage (Figure 4). Hence, any alteration in nAChR expression, function or activity may disturb crucial steps in neuronal organization. Furthermore, altered cholinergic signaling has effects on other neurotransmitter systems, including dopamine, noradrenaline and serotonin (Azam *et al*., 2007[48]; Xu *et al*., 2001[49]; Slotkin *et al*., 1987[50]).

Figure 4. Temporal and regional expression of nicotinic AChR subunit mRNA in developing human and rat brain.

Timeline for initial expression of mRNA for different nicotinic AChR subunits is illustrated. Given the diversity of nicotinic AChR subtypes as well as the differences in subunit composition and conformation (i.e., spatial arrangement of the different subunits within the receptor), mRNA expression is most often used to identify the potential for the presence of a specific nicotinic AChR subunit in different brain regions. However, it is important to note that expression of mRNA does not necessarily indicate the presence of functional receptors that incorporate that subunit. Abbreviations: GD, gestational day; PND, postnatal day. Figure from Smith *et al*., 2010[51].

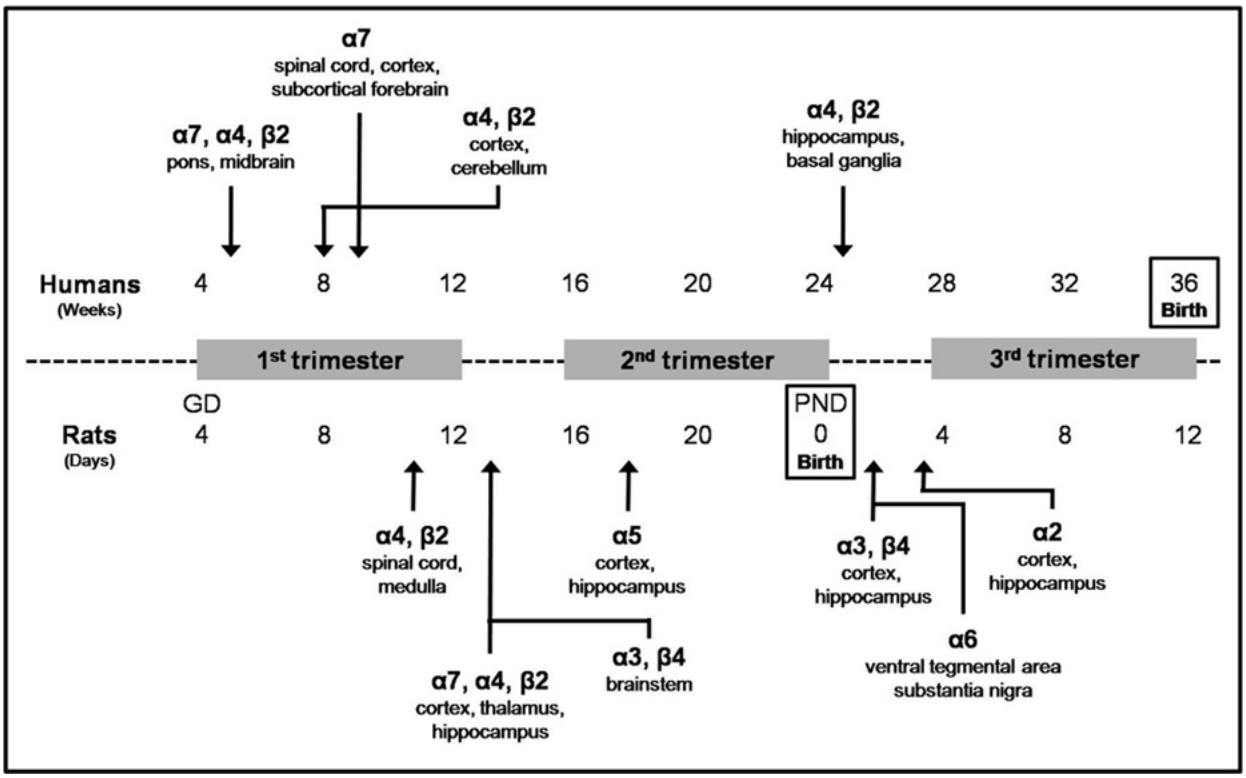

5.2 Altered nAChR expression

The α7nAChR subtype is essential for normal neurodevelopment. Increased or attenuated activity (eg. by neuroactive compounds) as well as up or down regulation of the expression have can be linked to several diseases. The α7 subunit gene is located in 15q13.1 locus, which is very sensitive to alterations, i.e., microdeletions or microduplications. Alterations in 15q13.1 in any direction (increase or decrease in functional receptors) may result in mental dysfunction, late onset of speaking, intellectual disabilities, risk of epilepsy and schizophrenia (Gillentine *et al.*, 2017[52]; Ziats *et al*.,2016[53]; Deutsch *et al*.,2016[54]). The α7nAChR subtype is not the exclusive product of the 15q13.1 locus. Nevertheless, there is a clear connection between impaired α7nAChR function and schizophrenia (Marcus *et al.,*2016[55]). Association between dysfunctional α7nAChR signaling and mental illness is further shown in different knockout mouse models that display phenotypes with depression-like symptoms (Zhang *et al.,*2016[56]) and impairments of cognitive and social behavior (Nacer *et al.,*2021[57]). Studies performed on α7 KO mice (8-14 weeks old) led to temporal processing deficits in the midbrain and auditory brainstem (Felix *et al.,*2019[58]). In 2009, Levin *et al*. Studied the effects on learning and memory in a radial maze test in β2 or α7 KO mice. The results

demonstrated that male β2 KO mice had choice accuracy impairment whilst the α7 KO mice also showed a significant impairment for both male and females (Levin *et al.*,2009[59]).

5.3 Signaling effects of prenatal exposure with nicotine

Slotkin (2008) reviewed the literature of nicotine exposure during pregnancy and evidence for abnormal neurodevelopment in animal models and humans (Slotkin, 2008[47]). Prenatal doses of nicotine that do not affect growth or induce secondary gross effects (most common endpoints in developmental studies), still have adverse effects on neurodevelopment and behavior (Navarro *et al*.,1989[60]; Eppolito *et al*.,2006[61]). Maternal smoking upregulates nAChR expression in brain of infants (Nachmanoff *et al.*, 1998[62]). Corresponding nicotine exposure in monkeys and rats give the same upregulation as a consequence of receptor desensitization (Slotkin *et al.*, 2002[63]). Disturbed nAChR signaling after prenatal nicotine exposure has also an impact on other neurotransmitter systems. nAChRs act as modulators of presynaptic transmitter release will thus change the signaling of multiple neurotransmitters at different developmental stages. For example, altered cholinergic signaling affects GABA and glutamate release and thus synaptic connectivity (Frazier *et al*.,1998[64]; Cheng and Yakel, 2015[65]. Prenatal nicotine exposure can affect signaling permanently and may alter the mood regulating neurotransmitter serotonin during adolescence (Slotkin *et al*.,2007[66]; Slotkin *et al*.,2006[67]).

5.4 Behavior/mental effects after prenatal nicotine exposure

Evidence for behavioral/mental effects after nicotine exposure is rich when related to studies on children with smoking mothers during pregnancy, however, co-exposure to multiple other problematic compounds confound the described findings.

6 Putative AOP

In order to integrate the various data generated for the purpose of the case study with existing mechanistic understanding, a putative AOP is proposed, since there is no adverse outcome pathway (AOP) described in AOP Wiki that explains nAChR binding as a molecular initiating event (MIE) leading to neurodevelopmental dysfunction as the adverse outcome (AO). However, the AOP describing chronic binding of antagonist to the glutamatergic ionotropic NMDA receptor during neurodevelopment, leading to attenuated Ca^{2+} influx, decreased release of brain derived neurotrophic factor (BDNF), impaired synaptogenesis and impaired learning and memory formation as AO is in progress (AOP:13 in AOPWiki.org) (Sachana *et al.*, 2018[68]). Based on the evidence of α7nAChR polymorphism and AOs like attention deficit syndrome (ADS), delayed mental development, schizophrenia and epilepsy together with the substantial evidence for nicotine as a neuroteratogenic compound, a putative AOP as a working hypothesis can be proposed. The AOP include binding to nAChRs (MIE), leading to activation of nAChR (KE1), leading to desensitization of nAChRs (KE2), leading to altered cellular phenotype (KE3), leading to altered neurodevelopment (KE4), resulting in delayed mental development, ADS, schizophrenia or epilepsy (AO). However, KE2 may be excluded in the case direct activation of nAChRs has impacts on KE3, KE4 and AO (Figure 5). In addition, gene expression changes can be considered as a possible KER between KE2 and KE3.

Figure 5. A putative adverse outcome pathway describing nAChR binding leads to impaired cognitive function and psychiatric diseases.

KE1 can lead to KE3 via KE 2 or directly. * Indicates endpoints not measured in this study.

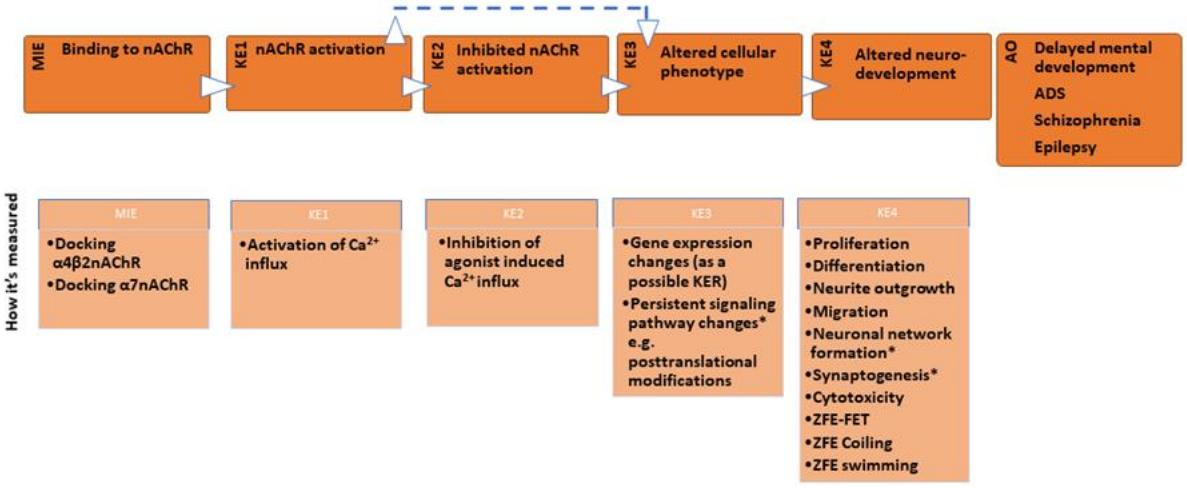

7 Data generation

7.1 Test systems

The MIE can be measured by docking models of acetamiprid on specific subtypes of the nAChRs and the KEs can be measured in cell models that display functional targets, i.e. nAChR subtypes that are relevant for neurodevelopment (Figure 5). Below, we describe the test systems that were used to measure the MIE and the KEs in the putative AOP. An overview of the test methods is provided in the Table 3 below.

Table 3. Overview of test methods.

	Key neurodevelopmental processes and cell survival						
Test Method	UKN2	UKN4	UKN5	NPC1-5 *	RoFA	TD42 iPSCs	SHSY5Y cells
Test System	neural crest cells	LUHMES (CNS neurons)	hiPSC neurons (PNS neurons)	*data from EFSA report (Masjosthusman et al.) reviewed and commented in report. Not in particular part of this IATA*	hiPSC differentiation into neuronal rosettes		
Endpoint 1	cytotoxicity	cytotoxicity	cytotoxicity		cytotoxicity	cytotoxicity	cytotoxicity
Endpoint 2	migration	neurite outgrowth	neurite outgrowth		rosette formation	-	-
SOP	attached	attached	attached		in work	attached	attached
publications	10.14573/altex.1605031	10.1007/s00204-013-1072-y	10.5966/sctm.2015-0108		10.1007/s00204-019-02612-5	10.1016/j.diff.2016.06.002	10.1007/s00204-021-03031-1

	Biochemical/Signalling			Transciptomic profiling of:	Zebrafish	In silico	
Test Method	CALUX assays	Calcium measurements			FET (OECD 236)	Docking	PBTK/QIVIVE
Test System	Several (31 human cell based assays in total)	LUHMES	SHSY5Y	neural crest, LUHMES, NEPs, TD42 iPSCs and SHSY5Y	Fish embryos	IFD; Schrödinger Release 2020-2	in silico
Endpoint 1	Cell signalling pathways	Ca whole well and single cell	Ca whole well		Lethality	representative docking poses	Internal exposure
Endpoint 2	Nuclear receptors	patch clamp	-		velopmental alteratio	-	-
SOP	attached	in work	attached		OECD TG 236	Induced Fit Docking protocol; Glide, Schrödinger, LLC, New York, NY, 2021; Prime,	Report attached
publications	https://doi.org/10.1002/9781118538203.ch28	10.1007/s00204-021-03031-1	10.1007/s00204-021-03031-1		https://www.oecd-ilibrary.org/environment/test-no-236-fish-embryo-acute-	https://doi.org/10.1021/jm050540c	Relevant references are described in the report

7.1.1 Docking models

For the structure-based approach, we focused on the major isoforms of the nAChRs in the human brain, α4β2 and α7. The heteropentameric subtype α4β2 had been resolved using cryo-EM-methodology and was retrieved from the protein data bank (rcsb.org; PDB-ID: 6cnk, 6cnj) (Walsh *et al.*,2018[45]). Regarding the homopentameric α7-subtype, we used a homology model which is based on a template of a chimeric structure of the extracellular ligand binding domain, which previously had been used as binding activity prediction model (Ng *et al.*,2018[46]). This was needed because there was no experimentally resolved structure when the study was conducted. However, a cryo-EM structure was released this year by Noviello *et al*. 2021[69]. The homology model was compared using superposition of the structures and resulted in an RMSD (root mean squared deviation) of 2.8 Angstroms which is less than the resolution of the structure (3.6 Angstroms). Both, the ligand Imidacloprid and the protein structures have been prepared for docking accordingly. We conducted molecular docking studies using the induced fit procedure in the software

package of *Maestro* (Schrödinger Release 2020-2, 2020), which integrates receptor flexibility up to a certain degree (Sherman *et al*.,2006[70]). The analysis of the docking poses was performed using protein-ligand-interaction fingerprint clustering and also the poses have been compared to conformations of neonicotinoids co-crystallized in model organisms (Lymnaea stagnalis; PDB-ID: 2zju) (Ihara *et al.,*2008[71]). More details about the docking approach can be found in the recent publications about the neonicotinoid pesticides (Loser *et al*., 2021a[13]; Loser *et al*., 2021b[14]).

7.1.2 LUHMES cells

The Lund human mesencephalic (LUHMES) cells were used as a test system to represent neurons with a dopaminergic phenotype. Via tetracycline induction LUHMES cells can be switched from a proliferating into a post-mitotic neuronal status in which cells further differentiate and grow a neuronal network, as described earlier in detail by Scholtz *et al*. 2011[72]. During differentiation cells change receptor composition including the expression of nAChRs (Fig. 6A). For example, gene expression of α4 and β2 subunits increase from day of differentiation 0 (D0) to D2. The LUHMES cell system can be used as a developmental system, targeting endpoints such as neurite outgrowth during differentiation as shown before Stiegler *et al*.(2011)[73]; Krug *et al*.(2013)[74]. Additionally, cells with a functional network can serve as a model to measure functional capacity, such as calcium signaling at present receptor types (Loser *et al*., 2021a[13]).

7.1.3 SH-SY5Y cells

The human SH-SY5Y neuroblastoma cells express functional muscarinic and nicotinic acetylcholine receptors (mAChR and nAChR, respectively) and they possess acetylcholine esterase activity. The expression of both metabotropic (M3) and ionotropic AChRs increases upon differentiation that is induced by all-trans retinoic acid (RA) (Figure 6B). When cultured in defined medium with N2 supplements and RA, the cells display neurochemical, structural and functional features of differentiated neurons. Hence, the cell model is useful for studies from proliferating neuroblasts to differentiated neurons. In the present study, 3 days-differentiated cells were exposed with compounds.

Figure 6. RNA-seq of cholinergic markers in LUHMES cells (A) and SH-SY5Y cells (B) during differentiation.
Figure A and B from Loser *et al*., 2021a[13].

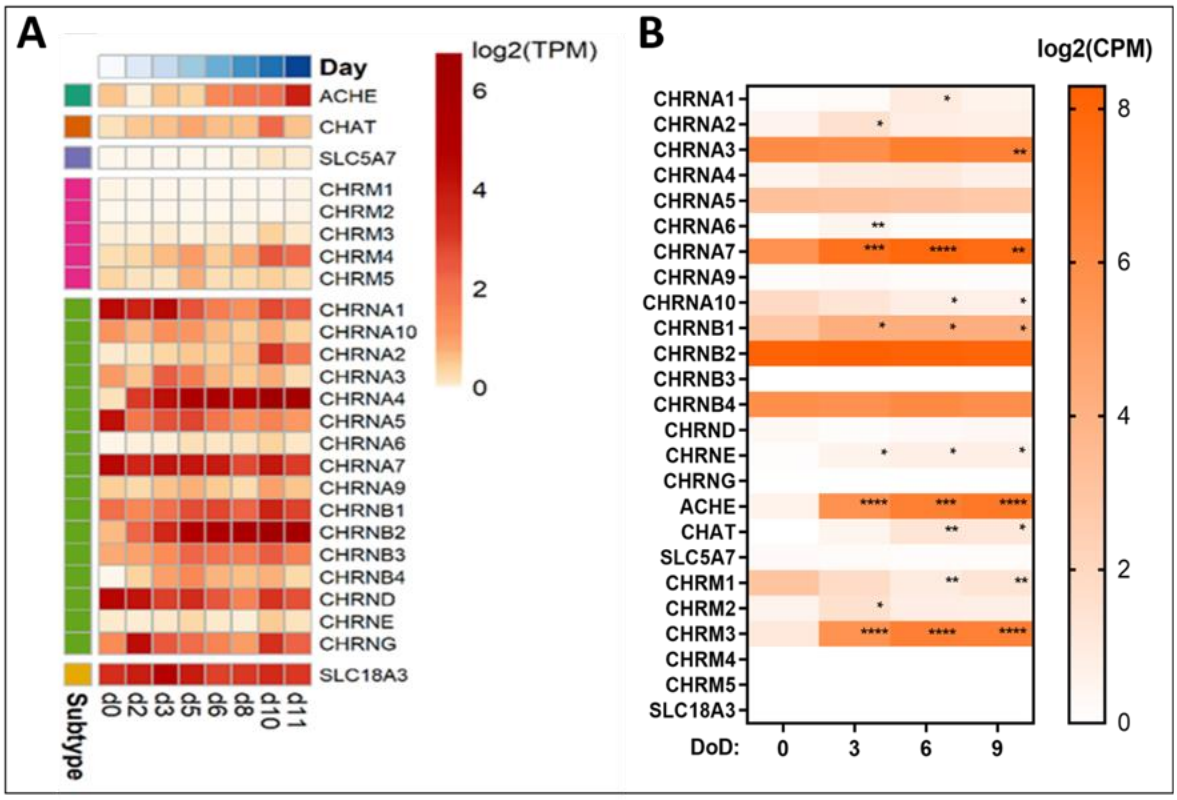

7.1.4 iPSC TD42

The test procedures describe the acute cytotoxicity of test compounds on human induced Pluripotent Stem Cell (hiPSC) -derived TD42 (terminally differentiated for 42 days) neural cultures using cell viability endpoint [Adenosine triphosphate (ATP) release measurement]. The test method is related to neural progenitor cell differentiation into glial and neuronal cells, mimicking the cytotoxic effect of compounds in early fetal stages (maturing neuro- and astrocytic toxicity at TD42) of neural development (developmental cytotoxicity). TD42 neuronal culture express specific subtypes of nicotinic acetylcholine receptors (AchRs), as seen in Figure 7.

Figure 7. Common neuronal nAChR subunits are expressed in TD42 samples.
The expression values were calculated as a relative amount of the mRNA versus the expression value of the Human Cerebral Cortex, which was set to 1. Samples were measured in triplicates.

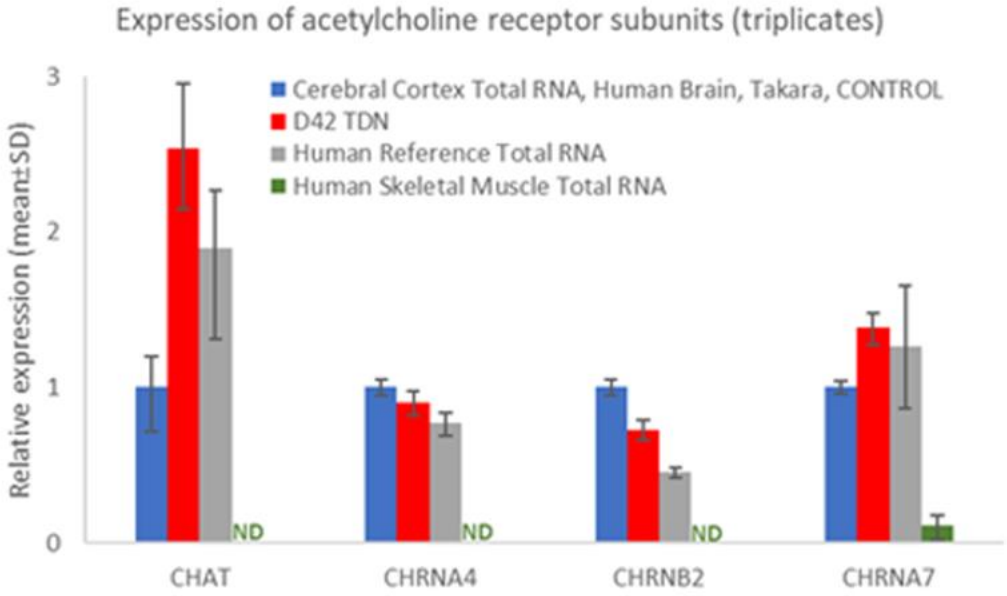

7.1.5 Neural crest cells

Neural crest cells (NCCs) represent a cell type during early neurulation, known for their characteristic to migrate throughout the body and capability to form different cell types. Here, NCCs were differentiated from the hiPSC line IMR90_clone #4 (WiCell, Wisconsin). Differentiation from hiPSC line IMR90 into NCCs was performed according to the modified protocol of Mica *et al*. 2013[75].

7.1.6 hiPSC-derived neuroectodermal progenitors

The hiPSC line iPSC EPITHELIAL-1 (= Sigma 0028) was used and differentiated following the differentiation protocol as described before Chambers *et al*.(2009)[76], with minor adaptations in differentiation factor concentrations as already used previously in Dreser *et al*. (2020)[77]. In more detail, hiPSCs were seeded as single cells and differentiated for a period of up to 12 days. The cell system represents an early stage of neurodevelopment, with strong SC marker expression in the beginning and a development to cells expressing markers typical for neuroectodermal progenitor cells, like PAX6 or OTX2 (Dreser *et al*. 2020[77]). Deregulated expression of these markers can be used as indicators for disturbed early neurodevelopment.

7.1.7 Peripheral/Sensory neurons

Sensory neurons for this study were differentiated from the hiPSC line SBAD2. SBAD2 cells were previously derived and characterized at the University of Newcastle from Lonza fibroblasts CC-2511, Lot 293971 with the tissue acquisition number 24245 (Baud *et al.,*2017[78]). Cells were differentiated as described earlier by Hoelting *et al*. (2016)[79] with the minor adaptations used in a previous compound screen (Masjosthusmann *et al.,2020*[9]).

7.1.8 Zebrafish embryo

The Fish Embryo Acute Toxicity (FET) test, in accordance with the Organization for Economic Co-operation and Development Test Guideline (OECD, 2013[80]), assesses the general teratogenicity of a compound to the developing zebrafish embryo between ±1.5 and ≤120 hours post fertilization (hpf). Thus, this assay was conducted to determine the 10 and 50% effect concentration (EC_{10} and EC_{50}, respectively), and endpoints were defined according to von Hellfeld *et al*., 2020[81](Figure 8A). Medium samples at 120 hpf, as well as freshly prepared samples, were collected and frozen in liquid nitrogen, before being sent for compound analysis. 120 hpf embryos for all FET test replicates were collected, washed in control medium, and frozen in liquid nitrogen, before being sent for transcriptome analysis.

Following the FET test, the compounds were tested in two behavioral assays to determine the effect of the compounds on the early neuro-developmental stages. The coiling assay was conducted between 24 and 48 hpf (Figure 8B) as described in Zindler *et al*., 2019[82], and examines the phase during which random neuronal firing turns into a distinct side-to-side coiling action within the chorion, considered to being vital for hatching. A more detailed description of the methods, along with the statistical analysis of all zebrafish embryo data can be found in the Annex I.

Figure 8. The zebrafish embryo assays conducted between 0 and 120 hpf.
A: The FET test in accordance with the OECD TG 236. Semi-static exposure of the embryos for 120h, with full medium renewal every 24h.

A

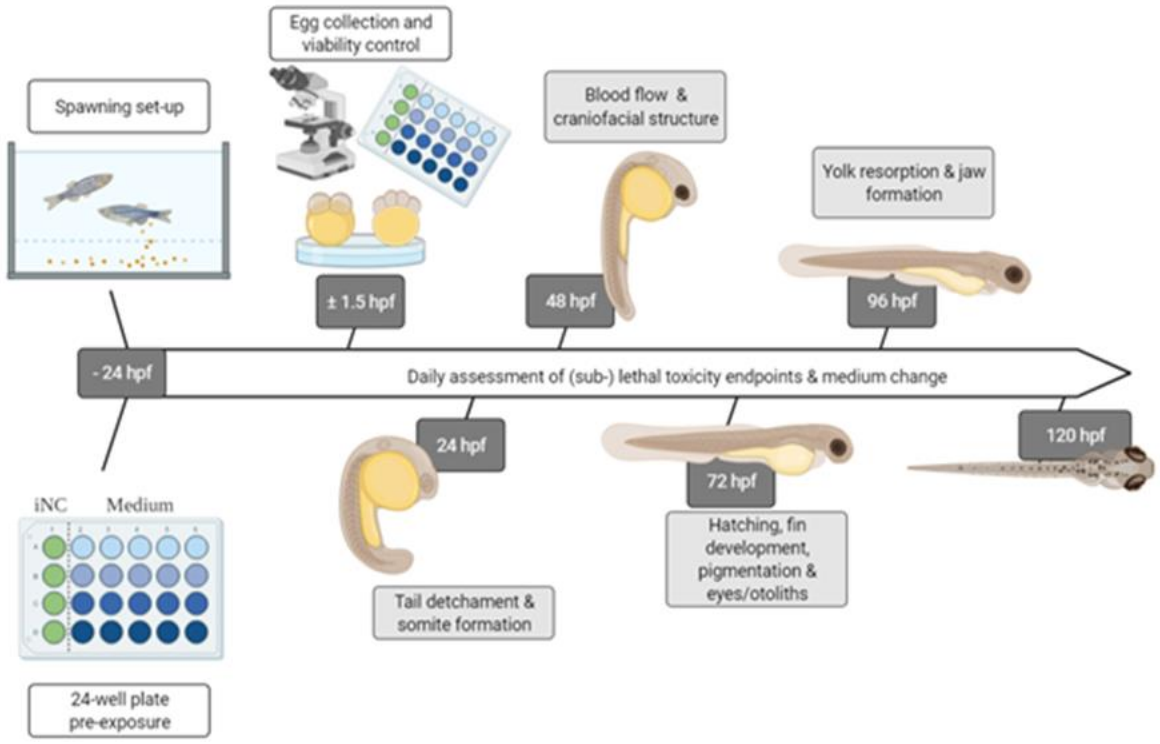

B: The coiling assay, with rearing conditions similar to the FET test, and video analysis of the burst frequency and duration between 24 and 48 hpf. The figure was adapted from von Hellfeld, (2021)[81]

B

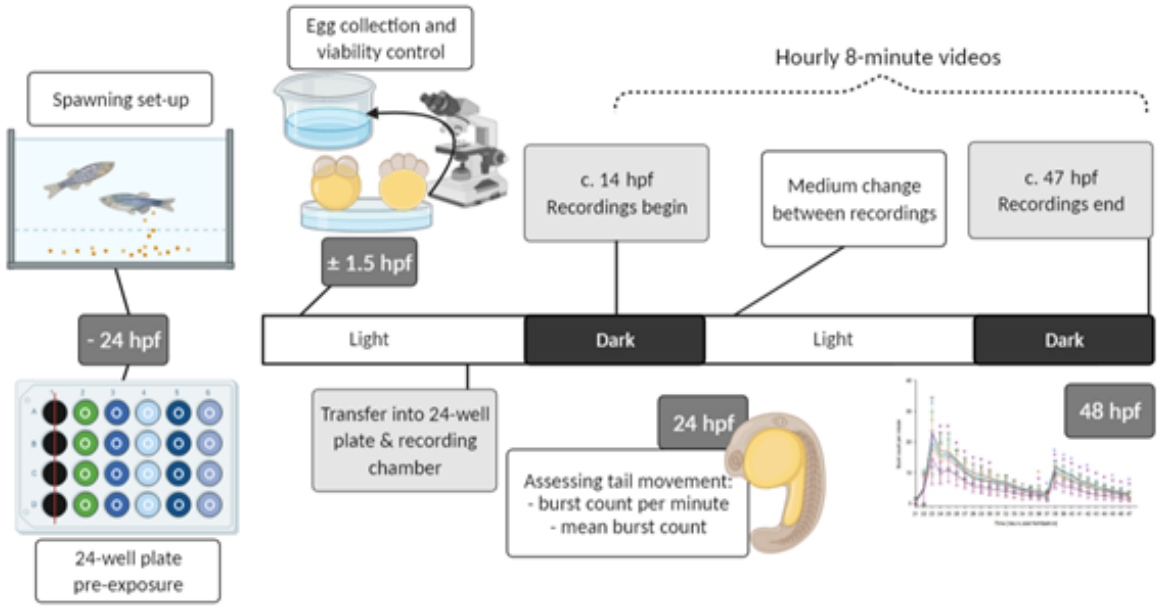

7.1.9 Other endpoints: CALUX reporter gene assays

From the CALUX® (Biodetection Systems) battery of *in vitro* reporter gene assays a panel of 31 human cell-based assays was used, each able to measure chemical interactions between a test chemical and a specific nuclear receptor or cell signaling pathway (Burg *et al.,2013*[83]). Exposure to the test compounds, dissolved at 0.1 M in DMSO, was performed for 24 h and at 1% (v/v) according to the assay procedure as described in DB-ALM protocol 197 "Automated CALUX reporter gene assay procedure". The concentration range used was 0.1 nM – 0.1 mM in 0.5 Log unit increments. The analysis consisted of technical triplicates and was performed twice as independent biological replicates. Lowest effect concentrations (LOEC) were derived per assay based on the background responses (see Figure 9 below). For nuclear receptor agonist assays, the LOEC was defined as the PC10 concentration in LogM, which is the concentration where the test compound causes an activation effect equal to 10% of the maximum effect elicited by the test's reference compound. For nuclear receptor antagonist assays, the LOEC was defined as the PC20 concentration, which is the concentration where the test compound causes an antagonist effect equal to 20% of the maximum antagonist effect elicited by the test's reference compound. For the stress pathway related assays which typically do not show sigmoidal dose-response curves, the LOEC was defined as the FI 1.5 concentration, which is the concentration where the test compound elicits pathway activation 1.5-fold above baseline.

Figure 9. Definition of LOECs for different assays within the CALUX panel.
A: nuclear receptor agonist assay; B: nuclear receptor antagonist assay; C: stress pathway assays (no sigmoidal dose-response).

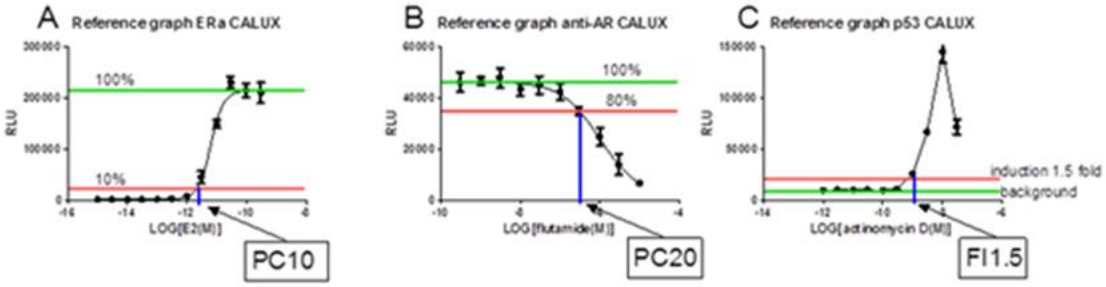

7.2 Methods to study KEs

7.2.1 KE1. Activation nAChR

Nicotinic AChR activation can be studied by monitoring changes in intracellular free Ca^{2+} concentration $[Ca^{2+}]_i$ using fluorescent dyes that bind Ca^{2+} (Figure 10).

Figure 10. Concentration-dependent effect of nicotine on the [Ca2+]i of LUHMES neurons.
The exposure to nicotine stimulated fast and transient increases in $[Ca^{2+}]_i$.

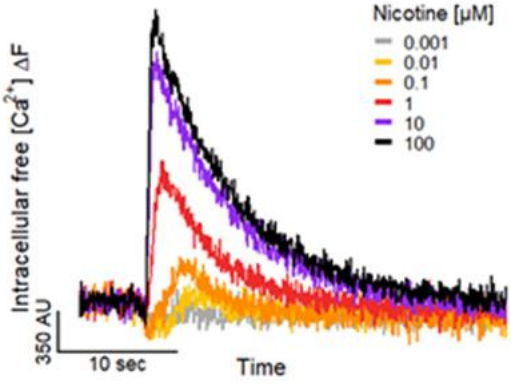

Ca^{2+}-imaging was performed using HT Functional Drug Screening System FDSS/µCELL (Hamamatsu Photonics) at nominal 37 °C. The FDSS/µCell system enables the indirect recording of changes of $[Ca^{2+}]_i$ via a Ca^{2+}-sensitive fluorescent dye. The fluorescence signal of a complete 384-well plate is acquired at once with a high-speed and high-sensitivity digital ImagEM X2 EM-CCD camera (Electron Multiplying Charge-Coupled Device, Hamamatsu Photonics), but with limited spatial resolution. Therefore, the software only determines the mean fluorescence signal of each well rather than of individual cells. Cells were pre-incubated with Cal-520 AM (AAT Bioquest) at a concentration of 1 µM for 1 h at 37 °C. For recording, the medium was exchanged by a buffer solution containing [mM]: 135 NaCl, 5 KCl, 0.2 $MgCl_2$, 2.5 $CaCl_2$, 10 HEPES, and 10 D-glucose, pH 7.4. Test compound application was executed after obtaining a 1.5 min baseline recording. Where applicable, a second application was executed 4.5 min after the first application. The total recording never exceeded 8 min.

Changes in $[Ca^{2+}]_I$ in SH-SY5Y cells were analyzed over time by measuring FURA-2AM fluorescence in a semi-high throughput screening (HTS) plate reader (FlexStation II, MolecularDevices). The area under the curve of the ratio in fluorescence between Ca^{2+}-bound FURA-2 (ex 340 nm, em 510 nm) and free FURA-2 (ex 380 nm, em 510 nm) was monitored during 150 seconds after acute addition of the compounds. In the majority of the experiments, the allosteric α7nAChR modulator PNU-120596 was used to prevent rapid desensitization and to favor measurement of Ca^{2+} influx induced by the same receptor subtype.

7.2.2 KE2. Inhibition nAChR function (desensitization)

The inhibitory effect on nAChR activity (i.e. inhibition of agonist-induced Ca^{2+} influx) was analyzed in LUHMES and SH-SY5Y cells in the presence of receptor specific allosteric modulators as described above after pre-exposure with the target compound and acute addition of receptor agonists.

7.2.3 KE3. Altered intracellular Ca^{2+} signaling alters cellular phenotype

In order to assess if altered Ca^{2+} signaling results in an altered phenotype as a downstream consequence, which was supposed in the putative AOP, transcriptomic changes were analyzed. For this, iPSC TD42, neural crest cells, neural ectodermal precursors, SH-SY5Y and LUHMES cells were treated with nicotine and imidacloprid and analyzed using an RNA-sequencing method (TempO-Seq assay, by BioSpyder Technologies Inc.) (House *et al.,*2017[84]). Follow up experiments in SHSY5Y and LUHMES cells are currently being analyzed.

Other phenotypic alterations than gene expression profile was not investigated so far.

7.2.4 KE4. Altered gene transcription affects neurodevelopment (neuronal differentiation, migration, axogenesis, synaptogenesis and brain area organization)

Viability – SH-SY5Y cells

The cell viability was determined in SH-SY5Y cells after 24 hours exposure with nicotine, imidacloprid or desnitro-imidacloprid by the conversion of resazurin to resorufin in metabolically active cells (O'Brien *et al.,*2000[85]). Resorufin fluorescence was measured at excitation 540 nm and at emission 590 nm using a FlexStation II fluorometer (Molecular Devices).

Viability - iPSCs TD42

At BIOT acute cytotoxicity assay is a medium throughput assay. Cells were seeded in 96-well plates with cell density 90.000 cells/cm^2. After 42 days, media was changed to 100 µl media containing the appropriate concentration of test compound. This TD42 assay is suitable to detect synaptic toxicity of compounds on mature neurons and neurotoxicity on astrocytes. The technical steps were provided in a Standard Operation Procedure (SOP) document (see DB-ALM Protocol No. 207).

Figure 11. Exposure scheme for acute (72 hours) toxicity treatment of TD42 differentiated neurons and astrocytes

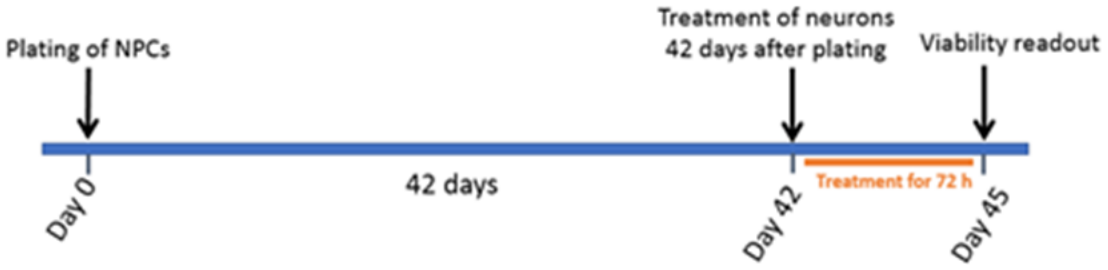

Cell viability is measured after 72 hours incubation time with the tested compounds by ATP viability assay. Endpoint values are the luminescent signals determined by the CellTiter-Glo® Luminescent Cell Viability Assay Kit (Promega, Cat. No. G7571).

Neurite outgrowth LUHMES cells (UKN4 assay)

LUHMES cells were differentiated for 2 days. On day 2 cells were reseeded and neurite outgrowth assay was performed as described earlier in detail by Krug *et al*. 2013[74] and Delp *et al*. 2018[86]. Shortly, cells were treated with compounds for 24h and allowed grow out neurites. After 24h, cells were live stained with H-33342 and calcein-AM and neurite area was measured using a high content imaging microscope (Cellomics ArrayScanVTI). In parallel, viability of cells was measured quantifying amount of double positive in relation to total cell number (single positive cells) (See scheme of assay in Figure 12).

Figure 12. The UKN4 neurite outgrowth assay using LUHMES cells.
A) Representative scheme of performance of the UKN4 method
B) Algorithmic readout of d3 neurites, indicating an image typical for a solvent control (left) and a positive test compound (right) (Figure A from Loser *et al*., 2021a[13], Figure B from Masjosthusman *et al*., 2020[9]).

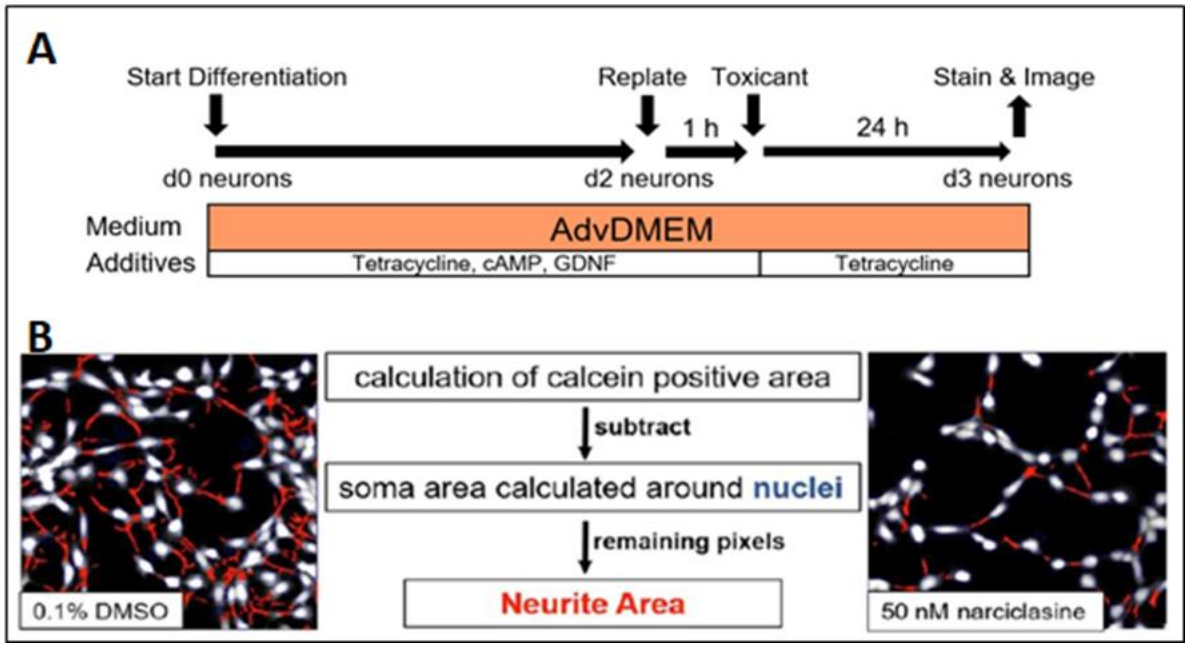

Neural crest cell migration (UKN2 assay)

NCCs were thawed and seeded for 4 days surrounding silicon stoppers in 96 well plates, as described in detail before by Nyffeler *et al*. 2017[87]. During their migration phase, cells were treated from day 3 to day 4 for 24 hours and live stained with H-33342 and calcein-AM and afterwards imaged using a high content imaging microscope (Cellomics ArrayScanVTI) (Figure 13). A program designed for this purpose was used to assess the number of cells which successfully migrated into the previously cell free area (http://invitrotox.uni-konstanz.de/RA/).

Figure 13. The UKN2 migration assay using neural crest cells
A) Representative scheme of performance of the UKN2 method
B) Algorithmic readout of cells migrated into the region of interest (ROI) indicating an image typical for a solvent control (far left), a positive test compound (left) and assessment of viability (right). Figure from Masjosthusman *et al*., 2020[9].

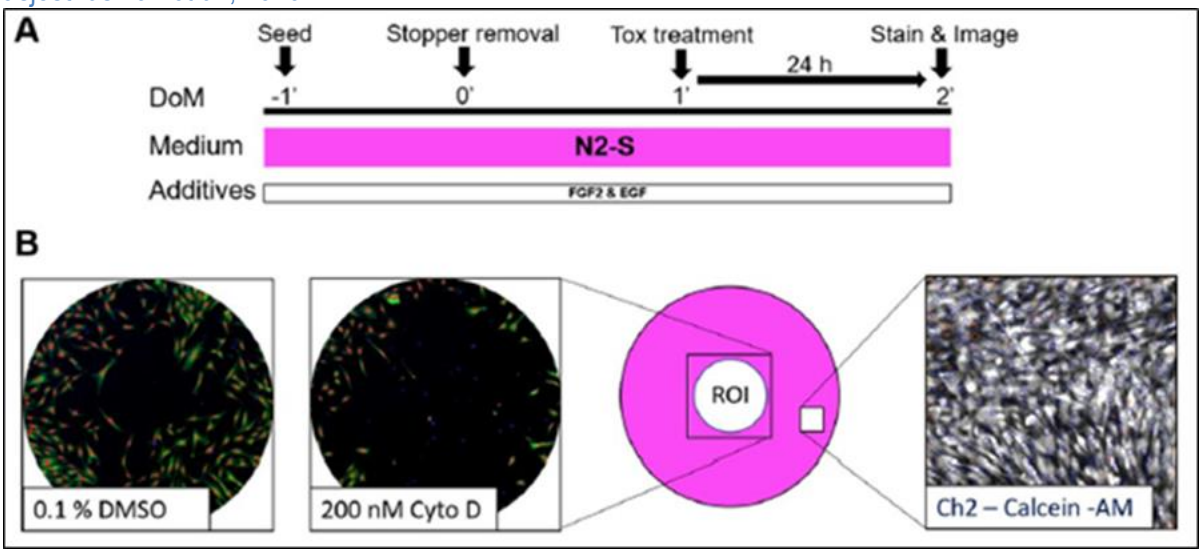

Neurite outgrowth sensory neurons (UKN5 assay)

Sensory neurons were thawed and seeded for 24h and exposed during this time to solvent or test compounds. Similar to the UKN4 test method (see above) cells were stained with H-33342 and calcein-AM to assess neurite area and viability in parallel. For detailed description of assay performance see Masjosthusman *et al.,* 2020[9].

NEP differentiation and rosette formation (UKN1 and RoFA)

Differentiation of hiPSC into neuroectodermal progenitors (NEP) and a rosette like phenotype was performed as described before Dreser *et al* 2020[77] with a shortened protocol as shown in Figure 14 below. Cells were treated for 96 hours with compounds and qPCR analysis was performed after 144 hours to assess correct differentiation into NEPs as an endpoint using marker genes (PAX6, OTX2). As a phenotypic endpoint, Rosette formation was assessed on day 12 via immunostaining as described earlier by Dreser *et al* 2020[77].

Figure 14. Differentiation and exposure scheme of the UKN1 test method from hiPSCs into NEPs and rosette like structures.

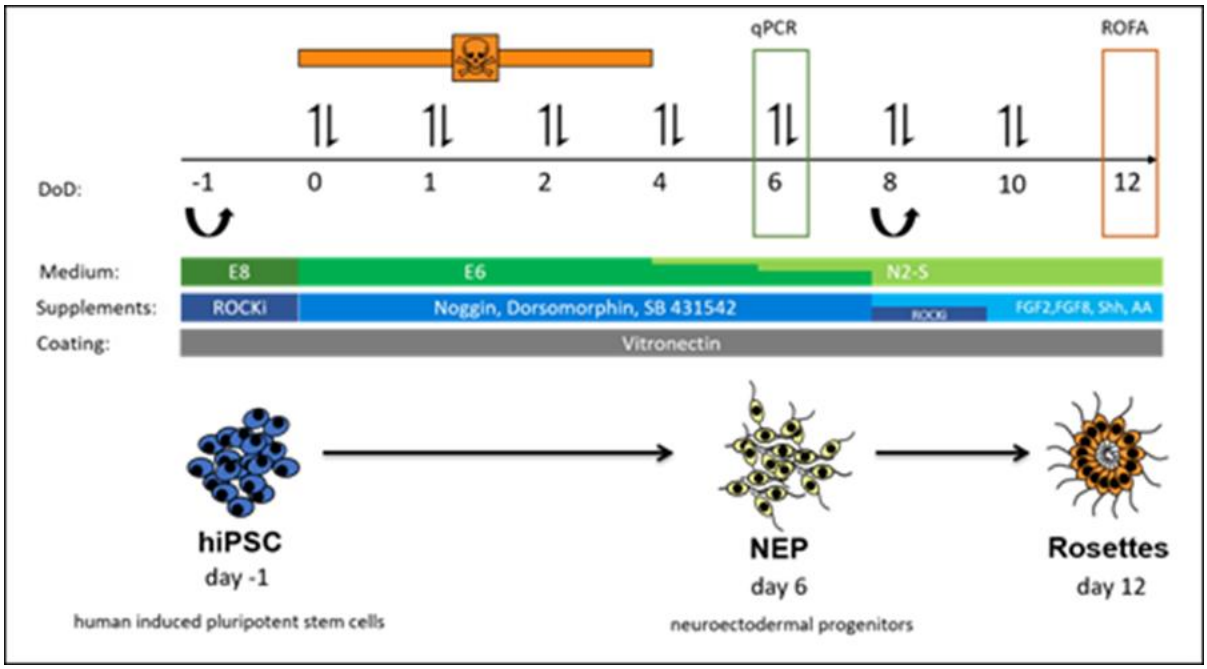

ZFE endpoints

FET test: Validity of a biological replicate was given, when no more than 10% of individuals in the negative control (untreated embryos) showed any developmental alterations, and at least 80% of the control group (and solvent control, where applicable) had hatched by 96 hpf. Moreover, validity was based on a minimum mortality of 30% in the 3,4-dichloroaniline (positive control) group (OECD, 2013[80]).

Behavioral assays: Due to the nature of the assays, only solvent controls were utilized in the coiling and swimming assays. No morphological developmental alterations in the controls were observed, and the data analysis of the treated groups were normalized to the controls.

7.2.5 Modelling of binding/docking to nAChRs

The main goal of docking and subsequent analyzing-methods such as clustering, in this study, are suggestions for structural explanations for differences in neonicotinoid activity on human nAChRs, that have been observed from cell experiments. Generally, the structures of the proteins and ligands of interest need to be prepared prior to the docking-procedure. Then we applied an induced fit docking protocol with extended sampling which is implemented in the software package of Schrödinger's *Maestro (Schrödinger Release 2020-2, 2020).* The poses of the ligands, Imidacloprid and Desnitro-imidacloprid have been clustered according to their interaction fingerprints with the protein and have been compared with binding modes from co-crystallized homologous structures. Analogous to the acetylcholine binding protein complex from *Lymnaea stagnalis* (Ihara *et al.,*2008[71]; Ihara *et al.,*2014[88]), an established protein surrogate for mammalian nAChRs, the neonicotinoid and its nicotinoid metabolite exhibit similar yet different binding orientations. The most striking difference lies within a flip of the imidazolidine ring. Desnitro-imidacloprid is lacking the electronegative functionality, and is therefore mimicking the binding mode of nicotine, while Imidacloprid is orienting the nitro group away from the central pore (Figure 15).

Figure 15. Nicotine (green carbon atoms, blue nitrogen atoms) has been co-crystallized in complex with human nAChR α4β2, superimposed with representative poses of desnitro-imidacloprid (pink carbon atoms) and Imidacloprid (orange carbon atoms, red oxygen atoms)

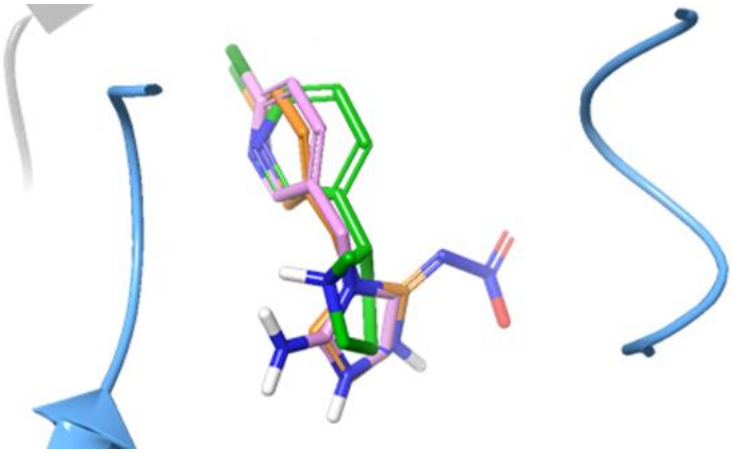

7.2.6 PBTK models

Separate PBK models were developed for Imidacloprid and desnitro-imidacloprid as the desnitro metabolite is also present in crops that have been treated with imidacloprid. The two models can be linked together if information on the rate and extent of desnitro-imidacloprid formation from imidacloprid becomes available.

PBK models for imidacloprid were constructed in the Simcyp Simulator V19 (Certara UK Ltd, Sheffield). To help with the parameterization of the PBK models metabolism of imidacloprid in human hepatocytes and binding to human plasma and blood was measured *in vitro*. Unfortunately, the metabolism of imidacloprid was below the limit of quantitation in the standard human hepatocyte suspension stability assay (LOQ ~ 3.86 µl/min/10^6 hepatocytes; Cyprotex unpublished observations) and in a low clearance assay format (LOQ ~0.143 µl/min/10^6 hepatocytes) to reliably determine the hepatic intrinsic clearance *in vitro*. In the absence of a measured value for protein binding in the rat a value was calculated assuming the same equilibrium dissociation constant (K_d) for human and rat albumin taking into account differences in the level of serum albumin in rat and human plasma.

PBK models were constructed using full body models in both rat and human where each organ of the body is modelled as a separate compartment. Distribution to tissues was modelled assuming perfusion limited distribution with the tissue:plasma partition coefficients being predicted based on physicochemical data using the method described by Rodgers and Rowland (2006)[89]. Initially the clearance of imidacloprid in the rat PBK model was determined based on the reported data from Kapoor *et al* (2014)[31]. A sensitivity analysis approach was used to find a range of clearance values in the rat whereby the simulated exposure of imidacloprid was less than the total radioactivity observed in plasma following oral dosing of ^{14}C- labelled imidacloprid to male rats.

Oral absorption of acetamiprid in rat and human models was predicted using a permeability value predicted from an *in silico* mechanistic permeability model (Sugano, 2009[90]) together with the solubility of imidacloprid. Oral absorption was predicted using the advanced, dissolution, absorption and metabolism (ADAM) model within the Simcyp simulator (Jamei *et al.,*2009[91]).

The human clearance of imidacloprid has not been defined. The clearance used in the model was calculated based on the predicted Vss and the reported half-life for excretion of deuterated imidacloprid in urine after oral dosing of 5 µg to human subjects (Harada *et al.,*2016[92]). The renal CL of imidacloprid was assigned based on the finding that 12-13% of the dose of deuterated imidacloprid was recovered

unchanged in human urine over 96 hours following oral administration of 5 µg of deuterated imidacloprid (Harada *et al.*,2016[92]). As different values of Vss and clearance can give the same half-life the effect of using different pairs of values was also investigated. All input parameters for imidacloprid are listed in Table 4 below.

Table 4. Input parameters for the PBK model for imidacloprid (rat and human)

Parameter	Value	Reference
Molecular Weight	255.7	Pubchem
Log P	0.57	
Compound Type	Neutral	
Blood:plasma ratio	1 (rat) 0.954 (human)	Measured Assumed
Fraction unbound in plasma	0.79 (rat) 0.724 (human)	Measured Calculated
Intestinal permeability		
MechPeff model (Ptrans,0 10^{-6} cm/s)	41.7	Sugano et al., 2009[90]
Solubility	0.61 mg/ml	Pubchem
Supersaturation Ratio	100	To ensure fa is consistent with observed data for radioactivity.
Distribution		
Vss	0.59 L/kg (rat) 0.49 L/kg (human)	Rodgers and Rowland, 2006[89]
Brain Kp	0.74 (rat) 0.78 (human)	Predicted
Clearance	Rat 5OH Vmax 159 pmol/min/mg Km 38.4 µM Additional Cl 6 ml/min Renal CL 0.58 ml/min Human HLM 0.228 µl/min/mg Renal CL 0.097 L/h	Kolanczyk et al. 2020[34] Based on excretion of unchanged imidacloprid in rat Adjusted to give a half-life of ~35 hours (in line with the urinary excretion data). Renal CL assigned based on recovery of deuterated imidacloprid in urine as reported by Harada et al., 2016[92]

8 Results (link to publications/BioStudies files)

8.1 MIE. Binding to nAChR (docking experiments)

Docking poses show that the guanidine moiety of desnitro-imidacloprid, which is embedded in the imidazolidine ring, is spatially aligning with the tertiary amine function of nicotine, as well as the pyridine rings. As the binding site residues of nAChRs compile a so-called “aromatic box” (Morales-Perez *et al*., 2016[93]), cation pi-interactions are likely to stabilize this nicotinoid binding mode (Dougherty, 2013[94]). This is contrary to Imidacloprid, which also aligns its pyridine ring but it points the nitro-guanidine moiety towards the tip of “loop C” and therefore accommodating a less buried binding mode. Moreover, we observed an additional binding mode of Imidacloprid that had previously been postulated for vertebrates in literature (Tomizawa *et al*., 2008[95]). In this inverted binding mode, the orientation of the neonicotinoid is reversed, compared to the so-called common binding mode that had been reported from co-crystallized homologous complexes. This means within the inverted binding mode, the nitro-group would be positioned, where the pyridine rings were aligning, and the chlorine-substituted pyridine ring was facing away from the central pore, so that Imidacloprid showed two distinct binding modes. Therefore, a mixture of different binding modes of Imidacloprid support the atypical concept of this binding hypothesis, associated with inferior potency of neonicotinoids on human nAChRs. Nevertheless, the metabolite desnitro-imidacloprid preferably exhibited a single binding mode, similar to the one of nicotine, which could give a rational for their comparable response in the cell experiments.

Figure 16. Docking poses of Imidacloprid in the model of human α7 nAChR.
Common binding mode is represented with orange carbon atoms, inverted binding mode is represented in purple carbon atoms, nitrogen, oxygen and chlorine atoms are depicted in blue, red, and green, respectively.

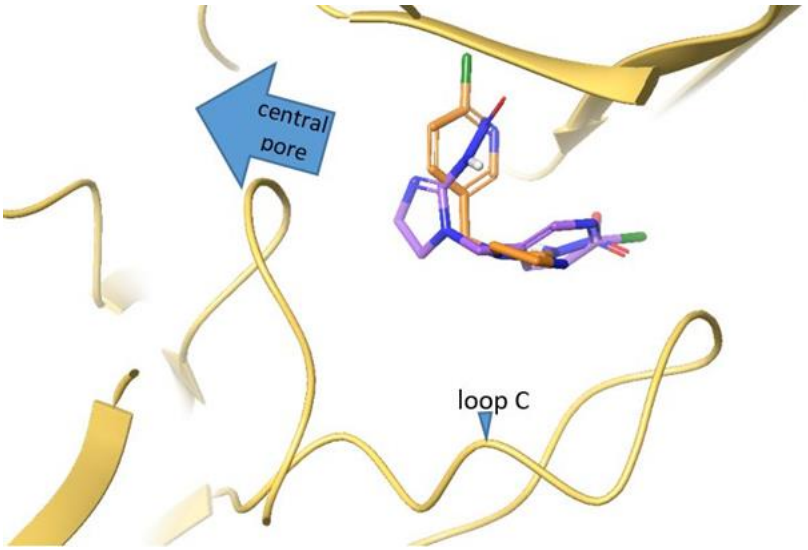

8.2. KE1. Activation of nAChRs

As previously stated, the α7 nAChRs are widely distributed in the nervous system and plays a major role during neuronal development. In order to investigate the effect of imidacloprid on the α7 nAChRs and to avoid rapid desensitization, Ca^{2+} measurements were performed in the presence of the α7 nAChR allosteric modulator PNU-120596. Here we found that PNU significantly enhanced the responses to imidacloprid in both LUHMES and SH-SY5Y cells (Figure 17). These results indicate that imidacloprid activates human α7 nAChRs.

Figure 17. Calcium influx measurements indicating nAChR activation in LUHMES and SH-SY5Y cells
A) Potentiation of imidacloprid (100 µM)-evoked $[Ca^{2+}]_i$ responses of LUHMES neurons in the presence of 10 µM PNU-120596, a positive allosteric modulator of the α7 nAChR (* = significant between recording of imidacloprid without PNU and negative control recording. # = significant between imidacloprid without PNU and imidacloprid with PNU recordings).
B) Imidacloprid induces Ca^{2+} influx in the presence of the allosteric modulator PNU-120596 (10 µM) in SH-SY5Y cells. This indicates that imidacloprid activates the α7 nAChR isoforms.8.3 KE2. Inhibition nAChR function (desensitization)

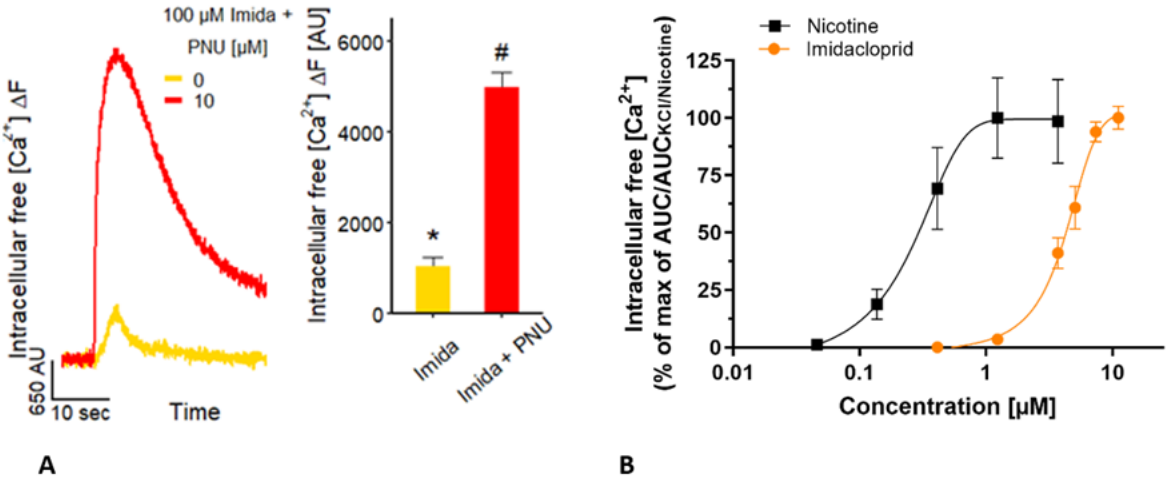

It is known for nAChRs that they can be desensitized, i.e. after a previous stimulus have an attenuated response. Therefore, the capability of imidacloprid and desnitro imidacloprid to desensitize nAChRs after a successful stimulus as shown in 8.2 above was tested. We found that increasing concentrations of imidacloprid lead to decreasing calcium influx in LUHMES cells treated subsequently with nicotine (Figure 18A and B). A similar effect but with a higher potency was found for the metabolite desnitro-imidacloprid with an IC50 of ~100 nM (Figure 18C). The effect of desensitization and a higher potency of desnitro imidacloprid compared to its parent compound were confirmed in SH-SY5Y cells (Figure 18D).

Figure 18. Desensitization nAChRs in LUHMES and SH-SY5Y cells.
A) & B) The pretreatment with imidacloprid negatively modulates the $[Ca^{2+}]_i$ responses of LUHMES neurons triggered by the subsequent, acute exposure to nicotine (3 µM) or ACh (3 µM). C) Pretreatment with desnitro-imidacloprid negatively modulates the $[Ca^{2+}]_i$ responses of LUHMES neurons triggered by the subsequent, acute exposure to nicotine (3 µM). D) Pretreatment with imidacloprid and desnitro-imidacloprid also negatively modulates the $[Ca^{2+}]_i$ responses of SH-SY5Y cells triggered by acute exposure to nicotine (11.1 µM)

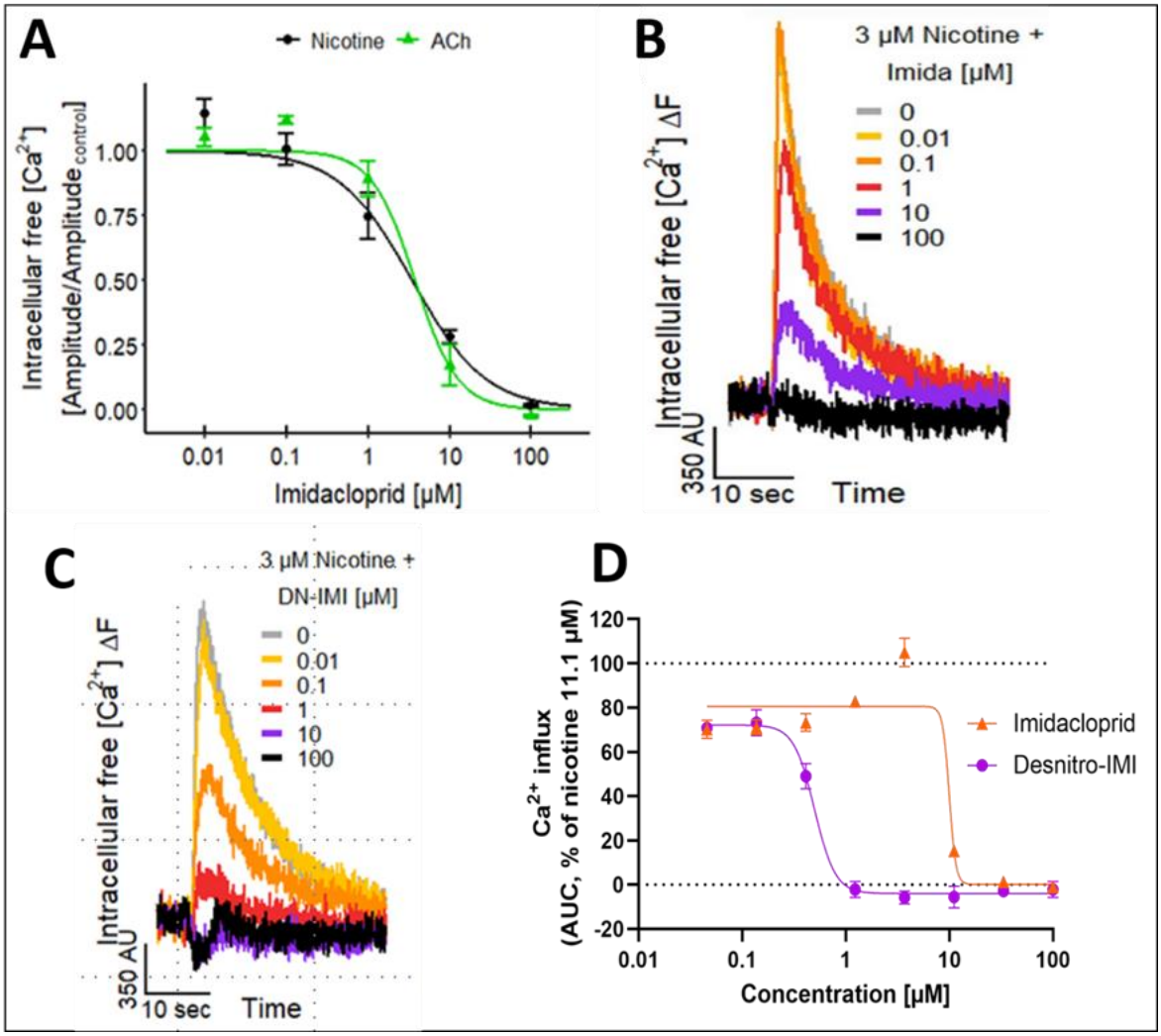

8.3 KE3. Altered intracellular Ca^{2+} signaling alters cellular phenotype

Intracellular calcium signaling regulates several cellular processes and influences the regulation of gene expression. Therefore, it was of interest to study possible differential gene expression after imidacloprid and desnitro-imidacloprid exposure. After 6 or 24 hours of exposure to non-cytotoxic concentrations of imidacloprid and desnitro-imidacloprid, there were only few or no differentially expressed genes (DEGs) seen. The SH-SY5Y cells indicated few statistically significant DEGs after exposure that were of interest for neuronal development. But from further analysis it could be concluded that this probably was due to the dynamic differential phase the cells were exposed during. Thus, the low effects seen cannot confirm

the hypothesis that nAchR activation by imidacloprid and desnitro-imidacloprid causes differential gene expression.

8.4. KE4. Altered gene transcription affects neurodevelopment (neuronal differentiation, migration, axogenesis, synaptogenesis and brain area organization)

8.4.1 Viability

Viability of SH-SY5Y

Neither imidacloprid (10 and 50 µM), desnitro-imidacloprid (10 and 50 µM) nor nicotine (1, 5 and 10 µM) affected cell viability in SH-SY5Y cells after 24 h of exposure (Figure 19).

Figure 19. Imidacloprid does not affect cell viability after 24 hours of exposure in SH-SY5Y cells

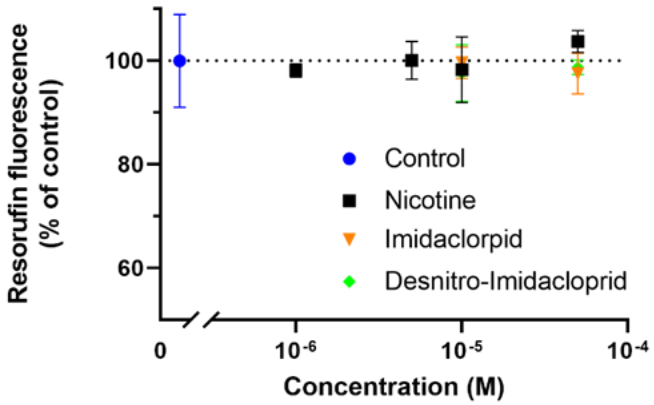

Viability of iPSC TD42

IPSC TD42 cells were exposed for to nicotine, imidacloprid and desnitro-imidacloprid and none of the compounds affected the cell viability after 72 hours (Figure 20).

Figure 20. Viability of 72 hours nicotine, imidacloprid and desnitro-imidacloprid treated cells. Concentrations of 0.01 to 100 µM had no impact on TD42 neuron viability.

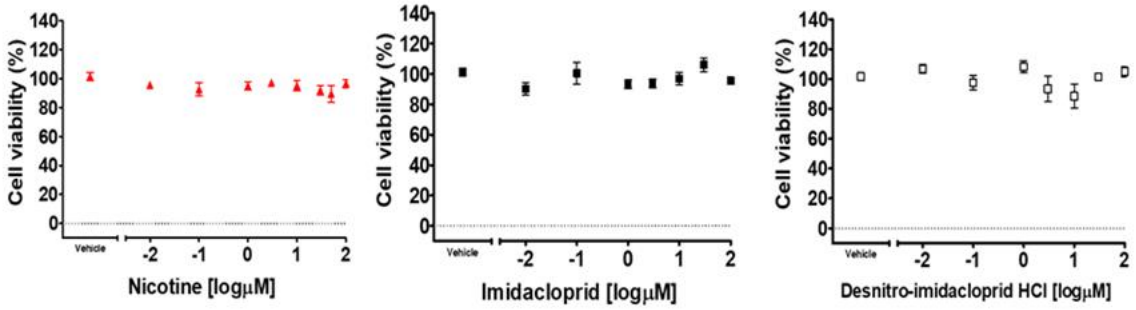

8.4.2 Neurite outgrowth, migration, differentiation and rosette formation

Cells were treated with concentrations of up to 100 µM. Viability of all 3 cells systems (LUHMES, sensory neurons, NCCs) was not affected with nicotine or imidacloprid (Figure 21below, Nicotine for UKN2 and UKN5 not shown). The assay specific endpoints i.e., neurite outgrowth in two cell systems and migration of NCCs were also not affected, neither with nicotine nor with imidacloprid.

Figure 21. UKN battery results including endpoint specific and viability measurements.
A) Neurite outgrowth and viability in LUHMES cells treated with nicotine
B) NCC migration and viability of cells treated with imidacloprid
C) Neurite outgrowth and viability in LUHMES cells treated with imidacloprid
D) Neurite outgrowth and viability of sensory neurons treated with imidacloprid.

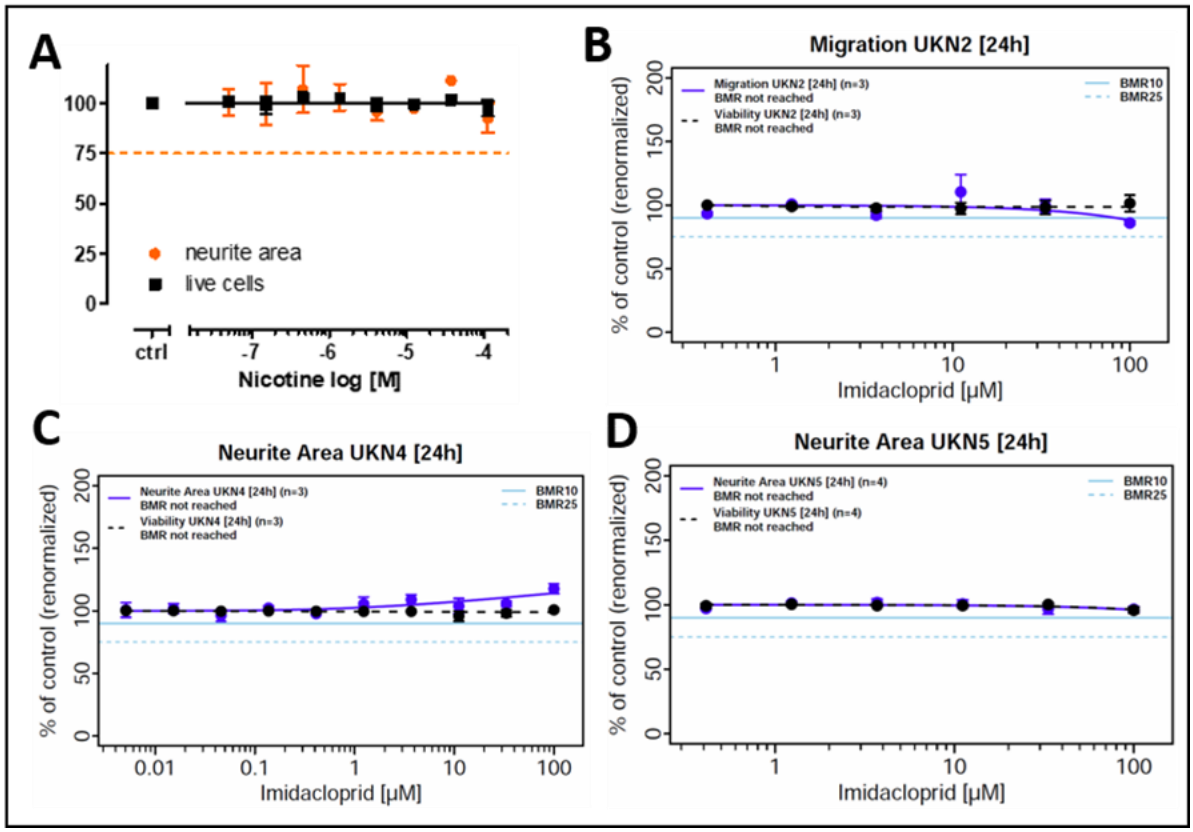

Differentiation and rosette formation of neuroectodermal precursor cells treated with nicotine and imidacloprid was not affected (data not shown).

To sum up, none of the cellular endpoints measured was affected by the compounds. Importantly, the cell systems which revealed positive results in KE1 and KE2 (SH-SY5Y and LUHMES cells) were not affected in viability.

Full DNT *in vitro* battery screen

In addition to the UKN2, 4 and 5 assays, imidacloprid was also part of an extended DNT *in vitro* battery project screen (Masjosthusmann *et al.*,2020[9]). Additional assays tested in this screening project are NPC1, NPC2, NPC3, NPC4 and NPC 5 (full method descriptions in report). Imidacloprid showed an effect in oligodendrocyte differentiation at concentrations below 20 µM.

It has to be considered that results from screenings should be handled with caution. Therefore, it would be important and should be considered to follow up on this screening alert. Especially, as evidence for KE4 remains poor so far.

8.4.3 ZFE endpoints

FET test: None of the compounds induced mortality during the FET test duration of 120 hpf. Table 5 outlines the EC_{10} and EC_{50} values obtained at 96 and 120 hpf. Imidacloprid exposure failed to induce any observable morphological alterations after 72 hpf.

Table 5. Effect concentrations (EC) of 10 and 50% for nicotine, or imidacloprid exposed zebrafish embryos as 96 and 120 hpf.
Values computed with ToxRat(R), given as mean (n=3), as outlined in Annex I. The table was adapted from von Hellfeld *et al*., (unpublished).

	96 hpf		120 hpf	
Compound	**EC_{10}**	**EC_{50}**	**EC_{10}**	**EC_{50}**
Imidacloprid	N/A	N/A	N/A	N/A
Nicotine	22.0	44.7	6.1	23.5

NA: No value could be computed at this time point, as none of the biological replicates showed any morphological alterations.

The observed developmental alterations in the FET test are listed in Table 6. Both compounds reduced the early spontaneous movement at 24 hpf, whilst nicotine was found to increase this parameter at exposure concentrations ≤ 12.5 µM. At 48 hpf, all compounds affected pigmentation, but nicotine failed to induce any further endpoints. An increasing number of endpoints were observed from 72 hpf onwards, with nicotine inducing more adverse effects than imidacloprid. At 96 and 120 hpf, imidacloprid induced no observable endpoints in the FET test, whilst nicotine affected the overall development (body length, craniofacial formation, and spinal cord), as well affecting the behavior at 120 hpf.

Table 6. All observed endpoints in the FET test, induced by nicotine (N) and imidacloprid (I).
The table was adapted from von Hellfeld *et al*., (unpublished)

Endpoint	**Developmental time-point [hpf]**				
	24	**48**	**72**	**96**	**120**
Spontaneous movement (-, =)	I, N				
Spontaneous movement (+)	N				
Delayed hatching			I, N	N	
Heartbeat (-, =, x)		I			N
Blood flow (-, =, x)		I			N
Spinal deformation (K, L)			I, N	N	N
Reduced body length			I, N	N	N
Edema		I	N	N	N
Otolith deformation					N
Pigmentation (-, =, x)		I, N	I, N	N	
Craniofacial deformation			N	N	N
Reduced yolk resorption				N	N
Tremor/Twitching					N
Increased late activity					N

Grey box: The respective endpoint cannot be observed at the given time point due to its link to a certain developmental stage.

Coiling assay: Both compounds induced behavioral changes in the coiling assay (Figure 22 and 24). Nicotine exposed embryos showed a delayed coiling onset, with the concentration dependent decrease of the mean burst duration (Figure 22A). Prior to the light cycle change at 37 hpf, all exposure concentrations >1.25 µM induced significant alterations. After the onset of the second dark phase (37.5 hpf), all exposure concentrations induced a significant reduction in mean burst duration. A clear concentration dependent decrease can be seen more clearly in the normalized data (Figure 22B). The burst count per minute was

also impaired by nicotine exposure (Figure 22C), where the 25 µM treatment group expressed an immediate lack of burst initiations, whilst the remaining groups showed a concentration-dependent delay in the early burst count peak (±24 hpf), as well as increasing the second peak around 37 hpf. The normalized data further outlines this behavior (Figure 22D).

Figure 22. The effects of nicotine on the early behavior of zebrafish embryos during the light/dark cycles of the coiling assay.

The mean burst duration [seconds]
(A) and normalized burst duration
(B), as well as the mean burst count per minute
(C) and normalized burst count
(D) between 21 and 47 hpf after exposure to various nicotine concentrations (n=3, 20 embryos per concentration/replicate).
Data regimes in A and C given as mean ± standard deviation. Normalized data in B and D was adjusted to the 0.1% DMSO treated solvent control group. Sections in the top bar indicate the phases of the illumination cycle. *: time point and concentration (in corresponding color) of significant difference to solvent control, a table of all significant *p*-values can be found in the Annex I. The figure was adapted from von Hellfeld *et al*., (unpublished)

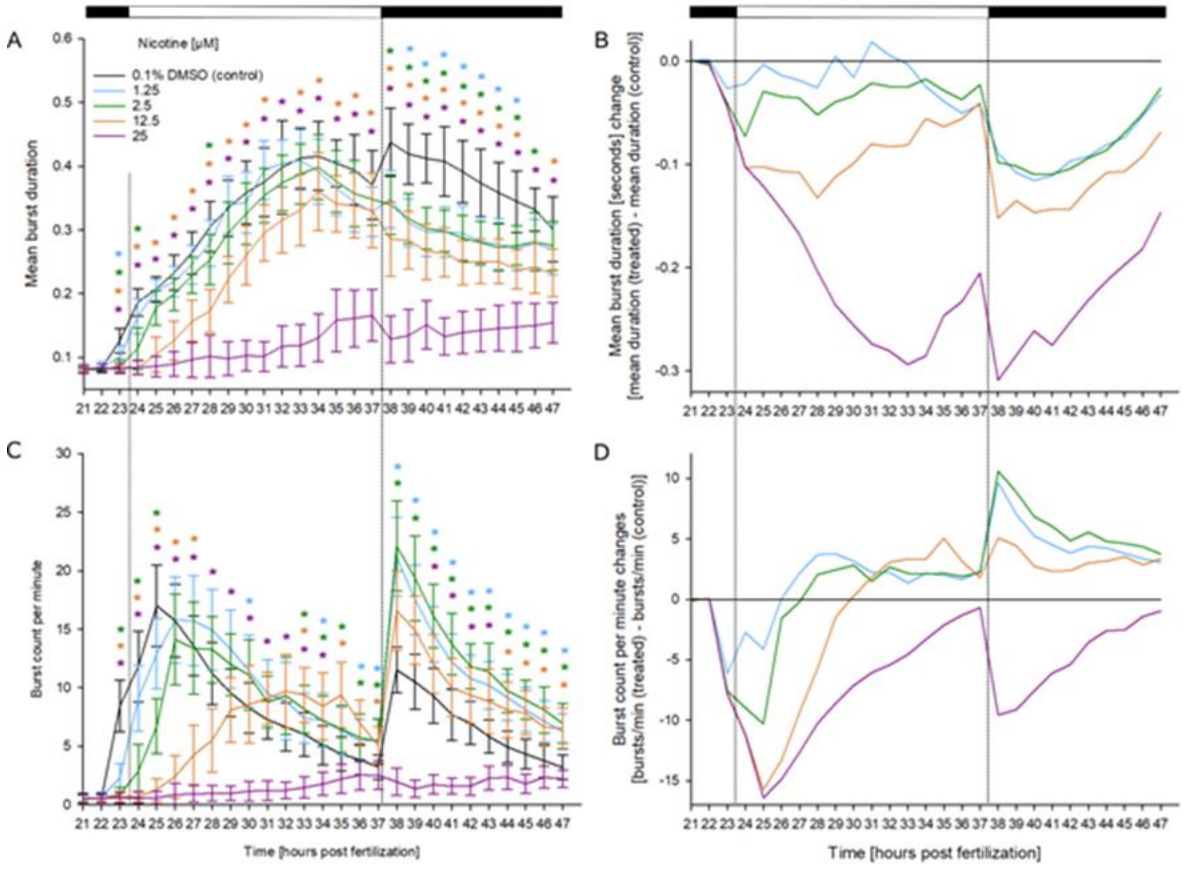

During early development, imidacloprid exposure significantly affected the burst duration behavior during light onset as well as causing a concentration dependent decrease in late coiling behavior (Figure 23A and B). The burst count per minute was less frequently significantly impacted by imidacloprid exposure. However, individuals also expressed a reduced response to the onset of light at 24 hpf. This is more pronouncedly visible from the normalized data (Figure 23C and D), as well as the following hyperactivity in both analyzed parameters.

Figure 23. The effects of imidacloprid on the early behavior of zebrafish embryos during the light/dark cycles of the coiling assay.
The mean burst duration [seconds]
(A) and normalized burst duration
(B), as well as the mean burst count per minute
(C) and normalized burst count
(D) between 21 and 47 hpf after exposure to various imidacloprid concentrations (n=4 until 37 hpf and n=1 post-37 hpf; 20 embryos per concentration/replicate).
Data regimes in A and C given as mean ± standard deviation. Normalized data in B and D was adjusted to the 0.1% DMSO treated solvent control group. Sections in the top bar indicate the phases of the illumination cycle. *: time point and concentration (in corresponding color) of significant difference to solvent control, a table of all significant p-values can be found in the Annex I. The figure was adapted from von Hellfeld *et al*., (unpublished)

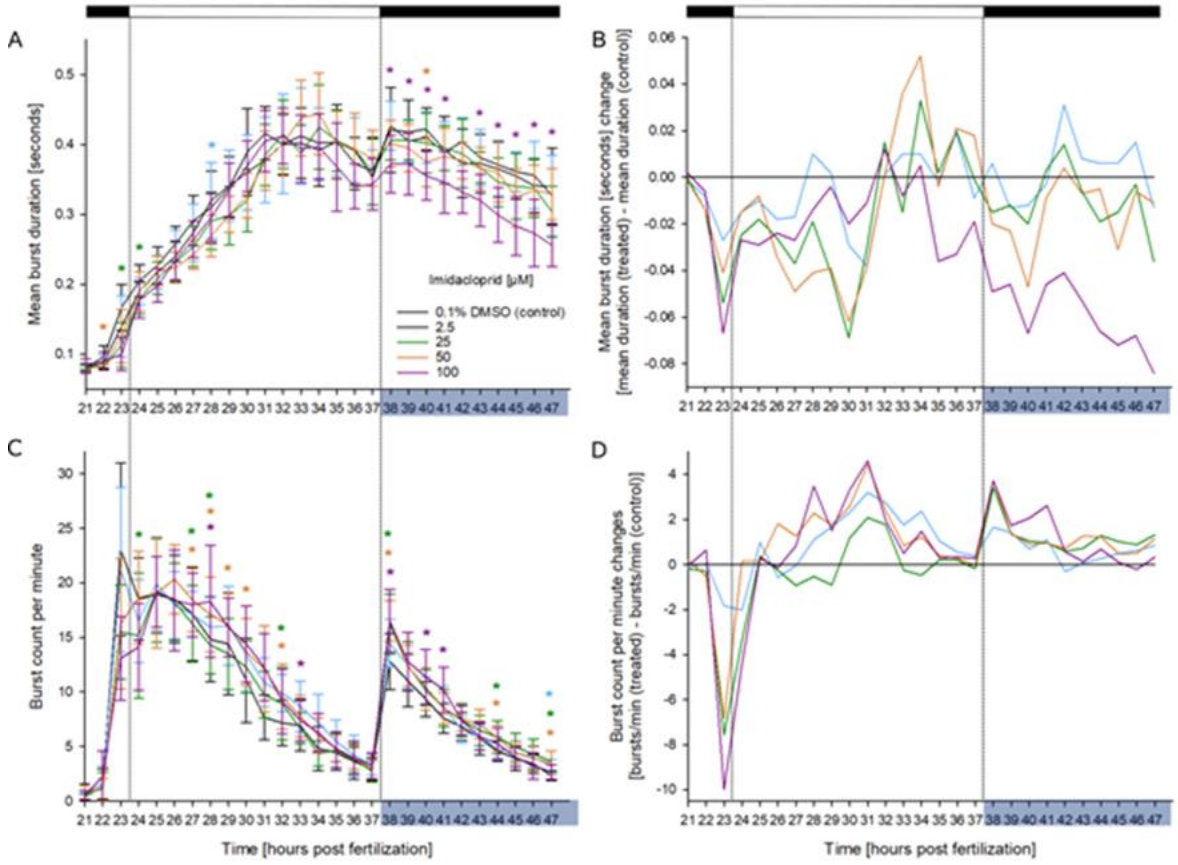

The relevance of these assays to the determination of DNT endpoints have previously been shown. Previous work has shown the strength of the zebrafish embryo as DNT model overall (Bailey *et al*., 2013[96]; De Esch *et al*., 2012[97]; Nishimura *et al.,*2015[98]; Tierney, 2011[99]), highlighting applicability beyond the FET test. Whilst early locomotor assays, such as the coiling assay, have been utilized frequently, the zebrafish has also lent itself to the assessment of other DNT aspects, such as learning and memory (De Esch *et al*., 2012[97]), as identical neurochemicals are involved in the vertebrate learning processes, which includes the zebrafish (Xu *et al*., 2007[100]). The locomotor behavior begins with the simple spontaneous coiling behavior

around 17 hpf (Saint-Amant and Drapeau,1998[101]), and is derived from a single neural circuit in the spinal cord Saint-Amant and Drapeau,2000[102]). The coiling assay lends itself to the assessment of early DNT, as an effect on the developing neural circuit is directly observable in the coiling behavior. The assay has been accepted as DNT-determining (Zindler *et al.,*2019[82]; Zindler, Beedgen and Braunbeck, 2019[103]; Zindler *et al.,*2020[104]; Selderslaghs *et al.,*2010[105]; Selderslaghs *et al., 2013*[106]; Weichert *et al.,*2017[107]; Velki *et al.,*2017[108]).

8.4.4 CALUX reporter gene assay results

Imidacloprid was analyzed on a full CALUX panel, consisting of assays detecting agonism or antagonism on nuclear receptors (ERα, AR, GR, PR, TRβ, LXR, PXR, PPARgamma, PPARdelta, RAR (agonism only), PPARα (agonism only) and AhR (agonism only)). The panel also contained several assays detecting activation of stress pathways (Hif1α, AP-1, ESRE, NFkB, Nrf2, p21, p53, TCF (incl inhibition)) and a cytotoxicity assay. Imidacloprid did not activate any of the assays up to the highest concentration tested (data not shown).

8.4.5 PBPK models outputs

The PBK model for imidacloprid was constructed initially in the rat. The distribution of imidacloprid to rat tissues was predicted using the algorithms proposed by Rodgers and Rowland (2006)[89]. The predicted brain:plasma ratio using this method is in line with experimental data in the mouse[32] and within 2-fold of the brain:blood ratio reported by Kapoor *et al*.(2014)[31]. Initial simulations using either *in vitro* metabolism data reported by Kolanczyk *et al*.(2020)[34] (not shown) or the calculated oral clearance of imidacloprid (0.83 ml/min) over-predicted the exposure of imidacloprid when compared to total radioactivity levels in the plasma of male rats dosed with 20 mg/kg ^{14}C-Imidacloprid (Figure 24). To bring the exposure of imidacloprid in line with the total radioactivity levels clearance of the compound was increased (Figure 24; Table 4). The clearance of Imidacloprid may be faster than the values used here as there is significant uncertainty in the true value of Imidacloprid clearance in the rat. The exposure and clearance of imidacloprid reported in female rats by Kapoor *et al*.(2014)[31] are inconsistent with the levels of total radioactivity reported in the DAR. Whether this represents a sex difference or is an effect of the corn oil vehicle used by Kapoor *et al*.(2014)[31], resulting in flip-flop pharmacokinetics and higher exposure is not clear. Although the delayed Tmax seen in the study by Kapoor *et al*.(2014)[31] is consistent with the second hypothesis.

Figure 24. Simulated (green line) concentrations of imidacloprid in plasma following an oral dose of 20 mg/kg to male rats.

Observed data (orange dots) are for total radioactivity after administration of 20 mg/kg doses of ^{14}C-imidacloprid. Data is taken from the DAR document Table B.6.1-22[109]. Panel B shows the data with the increased clearance values shown in **Table 3**.

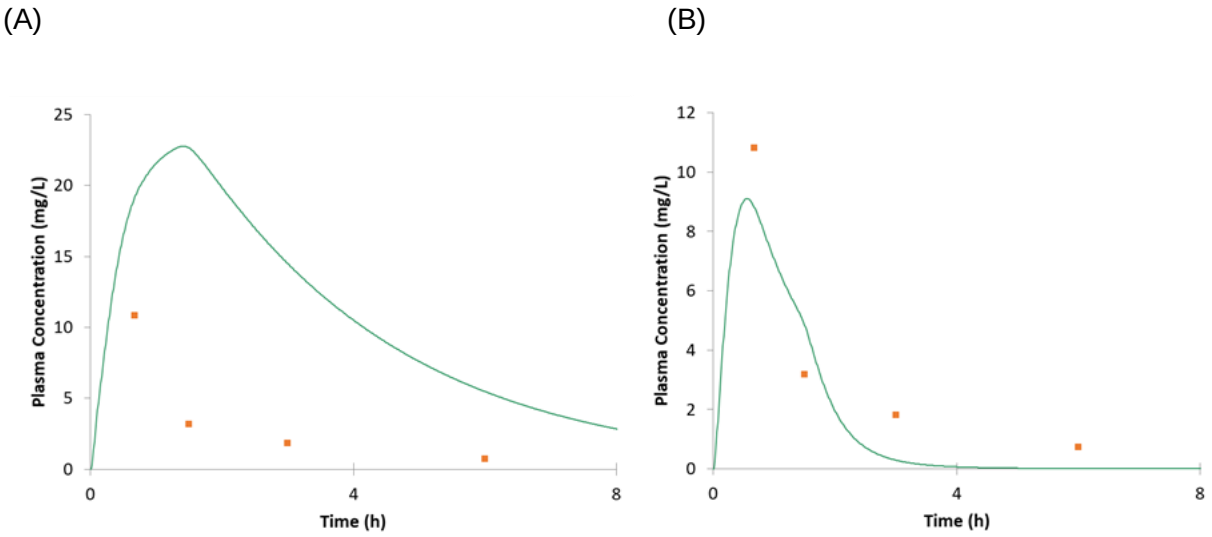

There is significant uncertainty in the input values for the rat PBK model and other values of Vss and combinations of Vss and clearance could equally give results consistent with the observed data which are based on total radioactivity after dosing of ^{14}C-imidacloprid. As is shown in Figure 25 as an example increasing the Vss by a factor of 2 or decreasing it be a factor of ~3 also produces results consistent with the observed data.

Figure 25. Simulated concentrations of imidacloprid in plasma following an oral dose of 20 mg/kg to male rats.

The green line shows simulations using identical input parameters to the simulation in Figure 24B (higher clearance value and kp scalar =1. The blue line shows a PBK model with a lower volume of distribution kp scalar =0.3. The grey line shows simulations with the same value of clearance but a larger volume of distribution. The Kp in each tissue apart from the brain was increased by a factor of 2. The brain distribution was unchanged ~0.75 to remain in line with measured brain:plasma ratio. Observed data (orange dots) are for total radioactivity after administration of 20 mg/kg doses of 14C-imidacloprid. Data is taken from the DAR document Table B.6.1-22109. Panel B shows the data with the y axis on a logarithmic scale.

(A) (B)

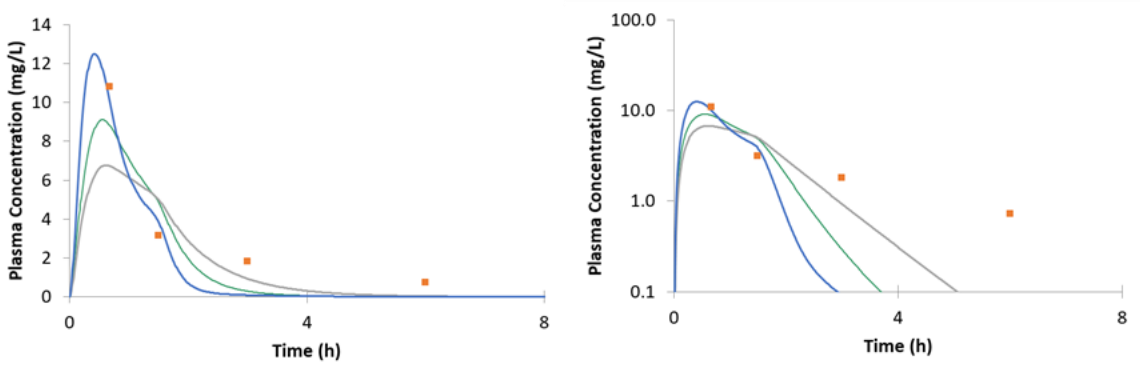

In humans the urinary excretion of deuterated imidacloprid has been measured following an oral dose of deuterated imidacloprid (Harada *et al.*,2016[92]). In the absence of other data, the data from Harada *et al*. was used to assess the performance of the PBK model under the assumption that the disposition of imidacloprid and the deuterated analogue are the same. Using the parameters outlined in Table 3 it is possible to produce a PBK model that is consistent with the observed data (Figure 26).

Figure 26. Simulated plasma concentration (A) and (B) urinary excretion of imidacloprid in humans after an oral dose of 5 μg imidacloprid.

Simulations were conducted in 100 North European Caucasian subjects (aged 20-50; 50% female). The green line represents the mean simulated data and the dashed black lines the 5th and 95th percentile of the population. The orange squares in panel B represent the observed data from Harada *et al*.(2016)[92].

(A) (B)

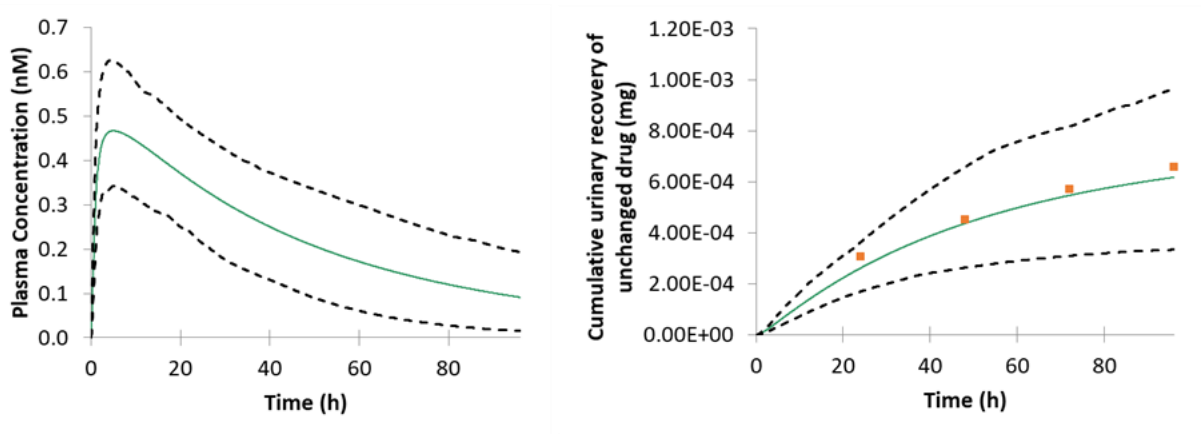

With only urinary excretion data after oral dosing available to verify the performance of the model there are different combinations of clearance and volume input parameters that can produce simulation results in line with the observed renal excretion data. This is illustrated in Figure 25 where the Vss used as input in the model is varied over a range of 0.3 to10 times the original values presented in Table 3. This was achieved by varying the kp scalar over a range of 0.3 to 10. At the higher values of kp scalar the brain:plasma ratio was kept constant at 0.75 to be consistent with the experimental data in mice. For each simulation, the renal excretion was kept constant at 12.7% of total clearance and the overall clearance varied to maintain a half-life of ~35 hours. The simulations were run in a population of individuals but only mean data is shown for clarity. As can be seen in Figure 27 varying the input parameters changes the plasma concentration of imidacloprid significantly but has minimal impact on the urinary recovery of the compound.

Figure 27. Simulated mean plasma concentration (A) and (B) urinary excretion of imidaloprid in humans after an oral dose of 5 μg imidacloprid.

Simulations were conducted in 100 North European Caucasian subjects (aged 20-50; 50% female). The different coloured lines represent different PBK models where the Vss and clearance were varied. The green line is the baseline model (Table 3) with a kp scalar of 1, the black line kp scalar = 0.3, blue kp scalar = 2, red, kp scalar =5, purple kp scalar =10. The orange squares in panel B represent the observed data from Harada *et al.*(2016)[92].

(A) (B)

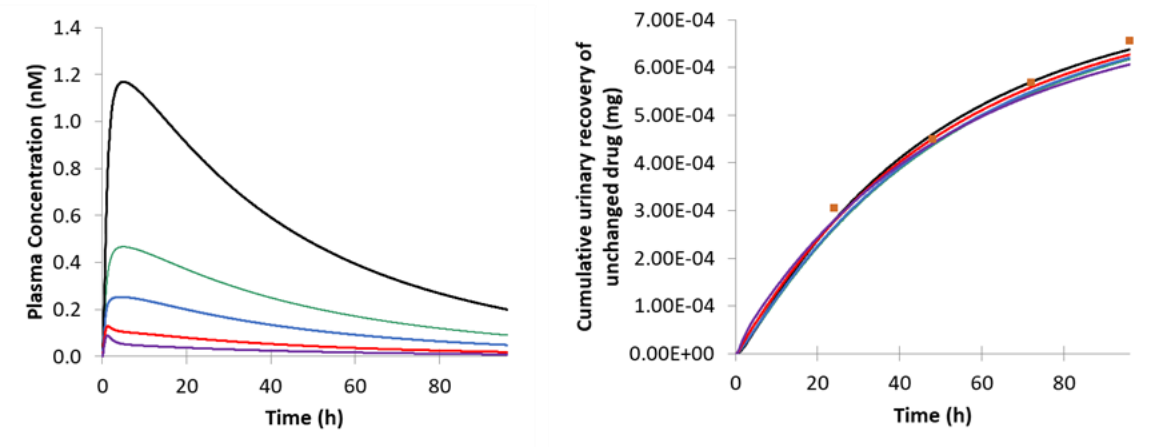

To keep the half-life constant in the simulations shown in Figure 27 the clearance is increased in parallel with the increasing volume of distribution. At the higher volumes (increased by 5 or 10-fold) the metabolic clearance needed within the model reaches a point when it should be observable in the *in vitro* assays that were conducted for the project. This suggests that the most likely combinations of parameters are when the predicted Vss of imidacloprid are <0.85 L/kg. This level of distribution within the body is consistent with a permeable compound that widely distributes through the whole-body water without extensively binding to tissues. This is consistent with the physicochemical and *in vitro* properties of imidacloprid. For instance, in the Caco-2 cell line the permeability of imidacloprid has been measured to be 21.6 x 10^{-6} cm/s consistent with a highly permeable compound (Brunet *et al.*,2004[110]).

The simulated exposure in humans (0.16/mg/kg/day; corresponding to a maximally expected level in the normal population) is shown in Figure 28. This intake scenario would lead to brain concentrations of 0.5-1.2 μM (Figure 28). Applying reverse modelling revealed, that a brain concentration of 2 μM imidacloprid (considered a point-of-departure from our *in vitro* studies) would be reached after an intake of 0.2 mg/kg body weight in the average population. Importantly, desnitro imidacloprid was found to be more than 10x more potent than imidacloprid in our studies.

Figure 28. PBTK modeling of imidacloprid concentrations in a human population exposure scenario.

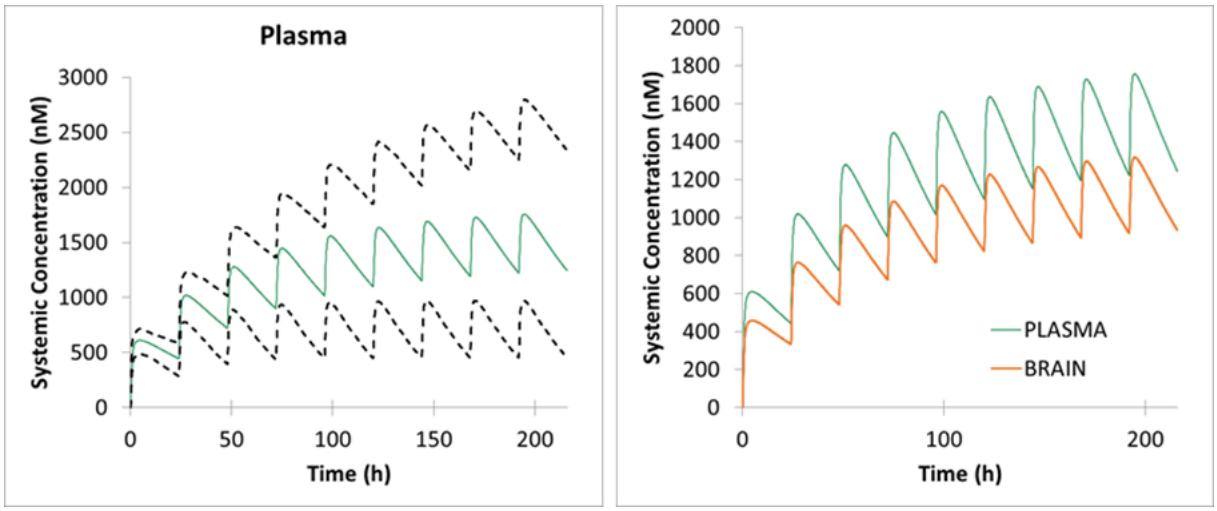

Also, simulations with a dose of 0.16 mg/kg/day were also undertaken in a population of pregnant female subjects the mean results were similar to those seen in the non-pregnant population of healthy volunteers (HV) (Figure 29).

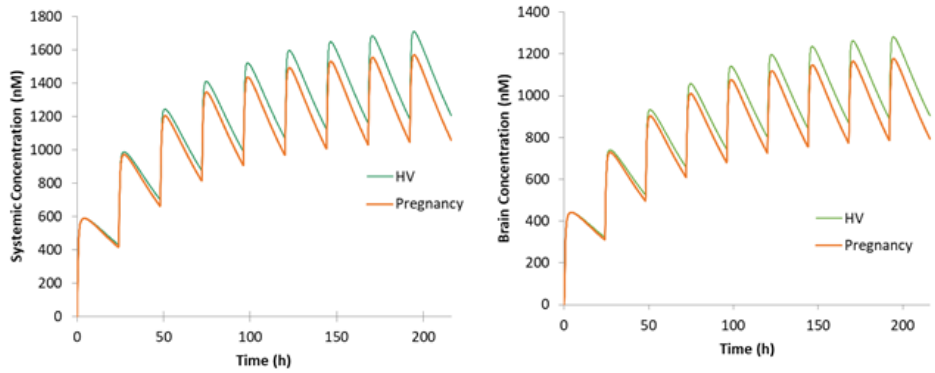

Figure 29. PBTK modeling of imidacloprid concentrations in pregnant and non-pregnant (HV) adult human population exposure scenarios

Although there is uncertainty in the enzymes involved in the metabolism of imidacloprid in human simulations were also conducted in a population of young children (age range 0.24 -0.26 years) exposed to a dose of imidacloprid of 0.16 mg/kg/day. Because the enzymology of imidacloprid metabolism is uncertain the change in metabolism of imidacloprid with age in children is also uncertain. To exemplify this different ontogeny profiles were simulated – assuming no ontogeny i.e. the enzyme level per mg protein is the same in adults and children and the fast, medium and slow ontogeny functions within the Simcyp simulator, Figure 30. If specific enzymes involved in the metabolism of imidacloprid are identified then the ontogeny of these specific enzymes can be incorporated in the simulations.

Figure 30. PBTK modelling of imidacloprid concentrations in adults (HV) and children (aged 0.24 – 0.26 years) exposed to an imidacloprid dose of 0.16 mg/kg/day.
In the children 4 different ontogeny profiles were simulated.

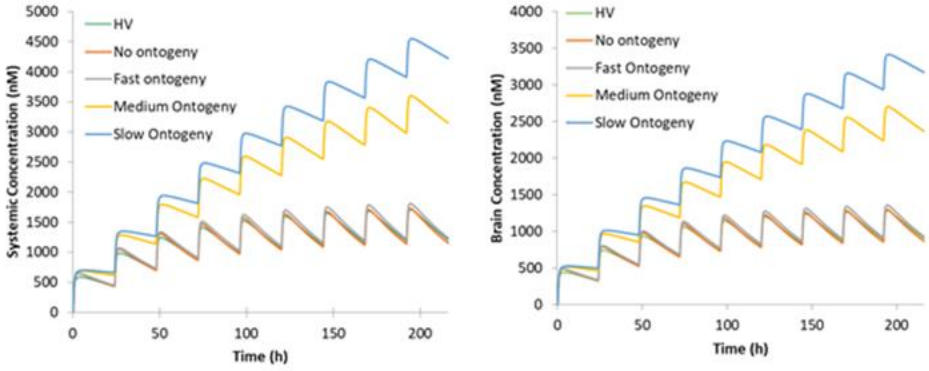

9 Uncertainty analysis

An uncertainty analysis is provided based on categories in an ordinal scale and is presented in Table 7 below. This is defined referring to the quality of the evidence generated/that was available supporting the assumptions of the case study and the overall weight of evidence and this is again related to the impact of the uncertainty on the hypothesis. For example, limited and poor quality evidence is likely to lead to larger uncertainty and vice versa.

Table 7. Uncertainty analysis of the IATA report highlighting the quality of evidence available and generated.

Factor	Uncertainty (low, medium, high)	Impact of uncertainty on hypothesis	Comment
Hypothesis	medium	medium	The hypothesis for the hazard characterization is based on established mode of action regarding the binding to the nAChRs as a pesticidal mode of action, although, the affinity towards the mammalian nAChRs is lower compared to insect nAChRs. However: -the prediction is based only on *in vitro* and *in silico* data, and -AO is an *in vivo* endpoint,
Used Approach (e.g. AOP/MOA, Defined Approach, workflow, read-across etc.)	High	high	The approach is based on analyzing and generating data anchored to a putative AOP. Here, the MIE and early KE's are widely recognized as dogma. However, the late KEs and importantly, the AO outcome are not well-characterized/specified. It should be noted that this is a general lack of knowledge for DNT AOPs.
Methods/assays used in the IATA	Medium	medium	Uncertainty of the assays/methods The different *in vitro* NAM methods used for addressing for characterizing the hazard do not have a validated regulatory guideline. However, they all have a consortium-wide reviewed description document according to Krebs et al. 2019. Importantly, the positive reference compound, nicotine has been tested simultaneously. The uncertainty of the individual assays/methods –Docking of a7 and a4◌ŋAChR. Uncertainty medium. Precise in defining the pockets and placing the molecules and is able to discriminate between neonicotinoid structures which are very similar. It is a well-established method. However, there is a high uncertainty regarding the use of this method as a model for the MIE. -Activation of Ca^{2+} influx. Low, seen in different assays, receptor expression checked -Inhibition of agonist induced Ca^{2+}influx. Uncertainty low since it was showed in two systems -Proliferation. Uncertainty low; well-established assays at partner institutes and SOP available, Masjostushmann et al 2020 -Differentiation. Uncertainty low; well-established assays at

			partner institutes and SOP available, Masjostushmann et al 2020 -Neurite outgrowth. Uncertainty low; well-established assays at partner institutes and SOP available, Masjostushmann et al 2020 -Migration. Uncertainty low; well-established assays at partner institutes and SOP available, Masjostushmann et al 2020 -Cytotoxicity. Uncertainty low; well-established assays at partner institutes and SOP available -hiPCS. Uncertainty low; well-established assay at partner institute. SOP and commercially available -CALUX reporters. Uncertainty low; well-established assay at partner, SOP and commercially available -ZFE FET test: Uncertainty low; well-established assay (in accordance with the OECD TG 236) at partner institute; SOP commercially available. -ZFE coiling assay: Uncertainty low; well-established assay at the partner institute, SOP not developed (assay execution varies between laboratories), programs and material commercially available; the assay has been accepted as DNT-determining -Transcriptomics data: low uncertainty due to no effect observed. The overall conclusions regarding the effects and potency of acetamiprid and the reference compound, nicotine, are comparable between the different labs and test systems, providing sufficient weight of evidence of low uncertainty for the overall outcome of the different test systems. However, overall the MoA may be dependent on precise developmental stage and neuronal phenotype and can be missed by some test systems. The *in silico* NAM method regarding the molecular docking has been externally reviewed in Loser et al. 2021; but is not well-established in the scientific as well as regulatory research. We consider the uncertainty medium. For the PBPK modelling standard procedures are followed according to OECD guidelines and includes sensitivity analysis to characterize the uncertainty.
Reference chemicals for performance evaluation of the assays/methods	Low	medium	Number of reference chemicals used for the performance evaluation of the assays and models is sufficient. Data has been shown related to nicotine, however, for characterization of the assays relevant well-established specific/general nAChRs agonist/antagonist have also been applied to further characterize the response in assays where activity was found as presented in Loser et al 2021
Quality of the data/information gathered and used in the IATA	medium	medium	Data/information gathered from the open literature was assessed in terms of relevance and reliability (bias) according to the protocol for the systematic review.
Concordance and weight of evidence of all data used for justifying the hypothesis	medium	medium	The gathered mammalian *in vivo* data does not show a consistent pattern regarding possible DNT effects. The available data have not examined similar endpoints between the experiments and also the experiments have done in different species. The ZFE data shows somewhat similar results throughout the assessed data, expressing the overall effect of acetamiprid on the organism. However, deviations are found, and experimental procedures were not always the same, hindering the comparison. It is shown that the acetamiprid can bind to mammalian a7 and a4○ņAChR and consistently induces Ca^{2+}-influx in

			separate assays. Also, like the reference compound nicotine and also other neonicotinoids (Loser et al 2021) imidacloprid/desnitro-imidacloprid, does not induce detectable functional effects in the assays regarding differentiation, proliferation, neurite outgrowth and migration. No molecular/cellular analyses were conducted with the ZFE, but endpoints correlating with nAChR inhibition were observed.
Overall uncertainty of the IATA	high	high	The main driving uncertainty relates to the lack of a well-established consistent adverse outcome as well as lack of understanding of later key events. However, the IATA establishes that imidacloprid/desnitro-imidacloprid inhibit nAChR activation in human cells at concentrations relevant for human exposures.

10 Conclusion

As described above, this case study presents an IATA with the purpose of characterizing the DNT properties of a neonicotinoid insecticide, imidacloprid and its metabolite desnitro-imidacloprid. The approach taken was to extract, appraise and assess existing human observational, *in vivo* and *in vitro* evidence related to DNT endpoints by on a search updated from the description in Sheets *et al*. (2016)[19].

In this context, no relevant human observational evidence was available. We identified 4 studies investigating effects of imidacloprid *in vivo*. Especially the study by Burke et al. indicated that exposure to imidacloprid at a low dose could result in behavioral deficits in offspring of female mice (Burke *et al*.,2018[23]). However, uncertainties remain, as most *in vivo* studies were lacking dose-response and suitable positive control data.

Most *in vitro* studies used concentration scenarios which can be considered non-relevant for human exposure. Kimura-Kuroda et al. 2016 indicated, that treatment with imidacloprid may alter the gene expression profile of rat neuronal cell cultures, but further investigations would be needed to decrease the high uncertainty of this study (Kimura-Kuroda *et al.,*2016[25]). The findings of Kimura-Kuroda et al. 2012, that imidacloprid triggers Ca^{2+} influx in rat cells, remains the *in vitro* study providing most mechanistic understanding (Kimura-Kuroda *et al.,*2012[11]). However, this study was reviewed already by Sheets et al. 2016 and the EFSA panel, and both came to the conclusion that further data underlining these findings is required (EFSA, 2013[10]; Sheets *et al*.,2016[19])

Therefore, further *in vitro* and *in silico* data has been generated, characterizing the effects of the compound in a battery of DNT *in vitro* test methods anchored to a postulated AOP and nuclear receptor activation. In addition, the toxicodynamic *in vitro* data has been contextualized with internal exposure predictions by PBPK modelling.

The further testing in the DNT IVB and additional systems/endpoint firmly establish that the imidacloprid/desnitro-imidacloprid neither nicotine affects these endpoints, neither do they show agonism or antagonism on various nuclear receptors, PPARα and AhR nor did the compounds activate stress pathways. However, imidacloprid has similar but less activity on nAChRs mediated Ca^{2+} influx in neuronal systems from nicotine, whereas desnitro-imidacloprid had similar potency as nicotine. These findings confirm previous findings and alerts raised by the publication of Kimura-Kuroda *et al*. 2012[11]. The uncertainties of this study and the early KE Ca^{2+} influx could be decreased, as the new data provides: I) human cell-based systems and confirmation in two different cell types II) Clear concentration dependent data III) Clear characterization and effects on nAChRs using sufficient tool compounds. Additionally, as a potential downstream KE, it was shown that imidacloprid and desnitro-imidacloprid have also the potential to desensitize nAChRs. This effect was found to occur at even lower concentrations.

The *in vivo* ZFE data reviewed in the present report outlines the strong effect of nicotine on the development and behavior of ZFE, whilst imidacloprid was found to show lower behavioral and developmental alterations. No lethal effects were observed throughout the FET test, and no EC values could be computed for imidacloprid exposed individuals due to the lack of effects observed apost-72 hpf. Whilst nicotine exposed ZFE showed a strong concentration dependent behavioral change in the coiling assay conducted for this report, imidacloprid exposure failed to induce more than sporadic coiling

frequency alterations, and only in the later stages of the assay was the coiling duration significantly impacted.

There still remain significant uncertainties regarding later KEs, including a specific adverse outcome. This major uncertainty is currently undergoing further investigations. As a first attempt, analysis of differential expressed genes in systems where imidacloprid/desnitro-imidacloprid and nicotine are active have been generated and is undergoing analysis. This could potentially point towards specific effect markers to investigate in relevant systems. Another possibility would be investigating activation/inactivation of signaling pathways.

In conclusion, imidacloprid/desnitro-imidacloprid induce Ca^{2+} signaling in neuronal systems mediated by nAChRs. Applying reverse modelling revealed, that a brain concentration of 2 µM imidacloprid, which was considered a point-of-departure from our *in vitro* studies, would be reached after an intake of 0.2 mg/kg body weight in the average population. This could potentially support a plausible mechanistic link to more firmly established human-relevant adverse outcomes.

11 Data Matrix

In this report, we have presented an IATA and postulated a putative AOP for nAChR binding as a MIE leading to neurodevelopmental dysfunction as the AO caused by the neonicotinoid pesticide imidacloprid and its metabolite desnitro-imidacloprid. The KEs proposed include activation of the nAChR leading to desensitization/inhibition which in turn results in transcriptional alterations due to increased intracellular calcium levels affecting functional processes such as differentiation and neurite outgrowth. We have generated data to fill data gaps connected to the AOP that are summarized in Table 8.

Table 8. Summary of data gap filling for imidacloprid and desnitro-imidacloprid.
LUHMES = neuron. SH-SY5Y = neuron. iPSC-derived neuronal culture = 42-days differentiated iPSC derived culture with astrocytes and different subtypes of neurons. ZFE = Zebra fish embryo. N/A = could not be determined as no effects were noted in all biological replicates. LCED = Lowest continuous effects dose (with 3 or more conseq. time points showing sign. at this concentration); NEPs = Neuroepithelial precursors; NCCs = Neural crest cells.

Summary of data gap filling					**Case 2**			
Type of chemical						Test compound	Test compound	Positive control
Chemical						Imidacloprid	Desnitro-imidacloprid	Nicotine
	Event	Assay						
in silico	Chemical specific	Similarity 3D		structural modeling a4ß2nAChR-AOP MIE1				
		Similarity 3D		structural modeling a7nAChR-AOP MIE2				
		Absorption						
		Distribution						
		Metabolism						
		Excretion						
	Key event	Tissue	Value	Measurement	Value			
in vivo	AO			Neuro/DART				
in vitro	KE1	LUHMES	EC50 (µM) mean± SEM	Ca^{2+} influx, non-a7 nAChR	EC50 (µM)	n.d.	6.56 ± 0.03	5.93 ± 0.05

		LUHMES	EC50 (µM) mean± SEM	Ca^{2+} influx, a7 nAChR (+PNU)	EC50 (µM)	-	6.45 ± 0.03	-
		SH-SY5Y	EC50 (µM) mean± SD	Ca^{2+} influx, a7 nAChR (+PNU)	EC50 (µM)	4.2 ± 0.45	0.48 ± 0.16	0.35 ± 0.10
			EC50 (µM) mean	Ca^{2+} influx, a7 nAChR		-	0,27	-
	KE2	LUHMES	IC50 (µM) mean± SEM	Inhibition of Ca^{2+} influx for 10 uM nicotine	IC50 (µM)	5.47 ± 0.10	6.94 ± 0.03	-
		LUHMES	IC50 (µM)	Inhibition of Ca^{2+} influx, a7 nAChR	IC50 (µM)	-	-	-
		SH-SY5Y	IC50 (µM)	Inhibition of Ca^{2+} influx for 11.1 µM nicotine, a7 nAChR	IC50 (µM)	9,98	0,49	-
	KE3	LUHMES	DEGs/BMC	Transcriptomic				
		SH-SY5Y	DEGs/BMC	Transcriptomic				
		iPSC-derived neuronal culture	DEGs/BMC	Transcriptomic				
		ZFE	DEGs/BMC	Transcriptomic				
	KE4	SH-SY5Y	BMC25 (µM)	Cytotoxicity (resazurin)	BMC25 (µM)	NE at 50 µM		NE at 10 µM
		iPSC-derived neuronal culture	BMC25 (µM)	Cytotoxicity (CellTiter-Glo® Luminescent Cell Viability Assay)	BMC25 (µM)	NE (BMC25>100µM)	NE (BMC25>100µM)	NE (BMC25>100µM)
		LUHMES	BMC25 (µM)	Neurite outgrowth (calcein-hoechst stain)	BMC25 (µM)	NE (BMC25>100µM)	NE (BMC25>100µM)	NE (BMC25>100µM)
		LUHMES	BMC25 (µM)	Cytotoxicity (calcein-hoechst stain)	BMC25 (µM)	NE (BMC25>100µM)	NE (BMC25>100µM)	NE (BMC25>100µM)
		ZFE	120 hpf EC10	FET	120 hpf EC10	N/A	N/A	0.6

			(µM)		(µM)			
		ZFE	LCED (µM)	coiling	LCED (µM)	100		1.25 (induced hyper- and hypoactivity)
		ZFE	LCED (µM)	swimming				
		Sensory neurons	BMC25 (µM)	Neurite outgrowth (calcein-hoechst stain)	BMC25 (µM)	NE (BMC25>100µM)	NE (BMC25>100µM)	NE (BMC25>100µM)
		Sensory neurons	BMC25 (µM)	Cytotoxicity (calcein-hoechst stain)	BMC25 (µM)	NE (BMC25>100µM)	NE (BMC25>100µM)	NE (BMC25>100µM)
		NEPs	Phenotypic	Differentiation and rosette formation	Phenotypic	NE (100 µM)	NE (100 µM)	NE (10 µM)
		NCCs	BMC25 (µM)	Migration (calcein-hoechst stain)	BMC25 (µM)	NE (BMC25>100µM)	NE (BMC25>100µM)	NE (BMC25>100µM)
		NCCs	BMC25 (µM)	Cytotoxicity (calcein-hoechst stain)	BMC25 (µM)	NE (BMC25>100µM)	NE (BMC25>100µM)	NE (BMC25>100µM)
	Other	Cytotox CALUX	BMC25 (µM) alt. Y/N	Cytotoxicity (U2OS cells)				
		anti-AR CALUX	BMC25 (µM) alt. Y/N	anti-androgenicity				
		CALUX panel	BMC25 (µM) alt. Y/N	all compounds negative up to 1 mM on all assays unless stated otherwise above				
		Reporters	BMC25 (µM) alt. Y/N	reporter target				
		Reporters	BMC25 (µM) alt. Y/N	reporter target				
		Reporters	BMC25 (µM) alt. Y/N	reporter target				

References

1. Organisation for Economic Co-operation and Development. *Test No. 426: Developmental Neurotoxicity Study*. (OECD Publishing, 2007).
2. *Test No. 443: Extended One-Generation Reproductive Toxicity Study*. (OECD, 2018). doi:10.1787/9789264185371-en.
3. Agency USEP: USEPA OPPTS 870.6300, Developmental Neurotoxicity Study. *EPA Office of Chemical Safety and Polution Prevention. Washington, U.S.* https://nepis.epa.gov/Exe/ZyNET.exe/P100IRWO.txt?ZyActionD=ZyDocument&Client=EPA&Index=1995 Thru 1999&Docs=&Query=&Time=&EndTime=&SearchMethod=1&TocRestrict=n&Toc=&TocEntry=&QField=&QFieldYear=&QFieldMonth=&QFieldDay=&UseQField=&IntQFieldOp=0&ExtQFieldOp= (1998).
4. Epa Ocspp, U. *NAFTA TECHNICAL WORKING GROUP ON PESTICIDES (TWG) DEVELOPMENTAL NEUROTOXICITY STUDY (DNT) GUIDANCE DOCUMENT*.
5. Bal-Price, A. *et al.* Recommendation on test readiness criteria for new approach methods in toxicology: Exemplified for developmental neurotoxicity. *ALTEX* **35**, 306–352 (2018).
6. Fritsche, E. *et al.* OECD/EFSA workshop on developmental neurotoxicity (DNT): The use of non-animal test methods for regulatory purposes. in *Altex* vol. 34 311–315 (Elsevier GmbH, 2017).
7. Crofton, K. M., Mundy, W. R. & Shafer, T. J. Developmental neurotoxicity testing: A path forward. *Congenital Anomalies* vol. 52 140–146 (2012).
8. Paparella, M., Bennekou, S. H. & Bal-Price, A. An analysis of the limitations and uncertainties of in vivo developmental neurotoxicity testing and assessment to identify the potential for alternative approaches. *Reproductive Toxicology* **96**, 327–336 (2020).
9. Masjosthusmann, S. *et al.* Establishment of an a priori protocol for the implementation and interpretation of an in-vitro testing battery for the assessment of developmental neurotoxicity. *EFSA Supporting Publications* **17**, 1938E (2020).
10. Scientific Opinion on the developmental neurotoxicity potential of acetamiprid and imidacloprid. *EFSA Journal* **11**, (2013).
11. Kimura-Kuroda, J., Komuta, Y., Kuroda, Y., Hayashi, M. & Kawano, H. Nicotine-like effects of the neonicotinoid insecticides acetamiprid and imidacloprid on cerebellar neurons from neonatal rats. *PLoS ONE* **7**, e32432 (2012).
12. M, T. & JE, C. Selective toxicity of neonicotinoids attributable to specificity of insect and mammalian nicotinic receptors. *Annual review of entomology* **48**, 339–364 (2003).
13. Loser, D. *et al.* Functional alterations by a subgroup of neonicotinoid pesticides in human dopaminergic neurons. *Archives of Toxicology* 1–27 (2021a) doi:10.1007/s00204-021-03031-1.
14. Loser, D. *et al.* Acute effects of the imidacloprid metabolite desnitro-imidacloprid on human nACh receptors relevant for neuronal signaling. *Archives of Toxicology 2021* **1**, 1–22 (2021b).
15. Brown, L. A., Ihara, M., Buckingham, S. D., Matsuda, K. & Sattelle, D. B. Neonicotinoid insecticides display partial and super agonist actions on native insect nicotinic acetylcholine receptors. *Journal of Neurochemistry* **99**, 608–615 (2006).
16. Tan, J., Galligan, J. J. & Hollingworth, R. M. Agonist actions of neonicotinoids on nicotinic acetylcholine receptors expressed by cockroach neurons. *NeuroToxicology* **28**, 829–842 (2007).
17. Casida, J. E. Neonicotinoids and Other Insect Nicotinic Receptor Competitive Modulators: Progress and Prospects. *Annual Review of Entomology* vol. 63 125–144 (2018).
18. National summary reports on pesticide residue analysis performed in 2018. *EFSA Supporting Publications* **17**, 1814E (2020).

19. Sheets, L. P. *et al.* A critical review of neonicotinoid insecticides for developmental neurotoxicity. *Critical Reviews in Toxicology* **46**, 153–190 (2016).
20. MB, A.-D. *et al.* Imidacloprid induces neurobehavioral deficits and increases expression of glial fibrillary acidic protein in the motor cortex and hippocampus in offspring rats following in utero exposure. *Journal of toxicology and environmental health. Part A* **71**, 119–130 (2008).
21. Kara, M. *et al.* Insecticide imidacloprid influences cognitive functions and alters learning performance and related gene expression in a rat model. *International Journal of Experimental Pathology* **96**, 332–337 (2015).
22. Liu, M. *et al.* From the Cover: Exposing Imidacloprid Interferes With Neurogenesis Through Impacting on Chick Neural Tube Cell Survival. *Toxicological Sciences* **153**, 137–148 (2016).
23. Burke, A. P. *et al.* Mammalian Susceptibility to a Neonicotinoid Insecticide after Fetal and Early Postnatal Exposure. *Scientific Reports 2018 8:1* **8**, 1–13 (2018).
24. Izumi, H., Ishimoto, T., Yamamoto, H. & Mori, H. Bioluminescence imaging of Arc expression in mouse brain under acute and chronic exposure to pesticides. *NeuroToxicology* **71**, 52–59 (2019).
25. Kimura-Kuroda, J. *et al.* Neonicotinoid insecticides alter the gene expression profile of neuron-enriched cultures from neonatal rat cerebellum. *International Journal of Environmental Research and Public Health* **13**, 987 (2016).
26. Nakayama, A., Yoshida, M., Kagawa, N. & Nagao, T. The neonicotinoids acetamiprid and imidacloprid impair neurogenesis and alter the microglial profile in the hippocampal dentate gyrus of mouse neonates. *Journal of Applied Toxicology* **39**, 877–887 (2019).
27. Wang, C. *et al.* Imidacloprid Exposure Suppresses Neural Crest Cells Generation during Early Chick Embryo Development. *Journal of Agricultural and Food Chemistry* **64**, 4705–4715 (2016).
28. E, F. *et al.* Mining the effect of the neonicotinoids imidacloprid and clothianidin on the chemical homeostasis and energy equilibrium of primary mouse neural stem/progenitor cells using metabolomics. *Pesticide biochemistry and physiology* **168**, (2020).
29. Christen, V., Rusconi, M., Crettaz, P. & Fent, K. Developmental neurotoxicity of different pesticides in PC-12 cells in vitro. *Toxicology and Applied Pharmacology* **325**, 25–36 (2017).
30. AO, O., E, T., R, M., S, S. & E, K. Optimization of the spontaneous tail coiling test for fast assessment of neurotoxic effects in the zebrafish embryo using an automated workflow in KNIME®. *Neurotoxicology and teratology* **81**, (2020).
31. U, K., MK, S., P, T., V, G. & LP, S. Disposition and acute toxicity of imidacloprid in female rats after single exposure. *Food and chemical toxicology : an international journal published for the British Industrial Biological Research Association* **68**, 190–195 (2014).
32. Ford, K. A. & Casida, J. E. Chloropyridinyl neonicotinoid insecticides: Diverse molecular substituents contribute to facile metabolism in mice. *Chemical Research in Toxicology* **19**, 944–951 (2006).
33. RA, D., DB, K. & JE, C. Identification of aldehyde oxidase as the neonicotinoid nitroreductase. *Chemical research in toxicology* **18**, 317–323 (2005).
34. RC, K., MA, T., BR, S. & JA, S. In vitro metabolism of imidacloprid and acetamiprid in rainbow trout and rat. *Xenobiotica; the fate of foreign compounds in biological systems* **50**, 805–814 (2020).
35. DA, S.-J. & JE, C. Imidacloprid insecticide metabolism: human cytochrome P450 isozymes differ in selectivity for imidazolidine oxidation versus nitroimine reduction. *Toxicology letters* **132**, 65–70 (2002).
36. DA, S.-J., WM, L. & JE, C. Neonicotinoid insecticides: reduction and cleavage of imidacloprid nitroimine substituent by liver microsomal and cytosolic enzymes. *Chemical research in toxicology* **15**, 1158–1165 (2002).
37. X, W. *et al.* Mechanism of Neonicotinoid Toxicity: Impact on Oxidative Stress and Metabolism. *Annual review of pharmacology and toxicology* **58**, 471–507 (2018).
38. H, H., M, T. & JE, C. Neo-nicotinoid metabolic activation and inactivation established with coupled nicotinic receptor-CYP3A4 and -aldehyde oxidase systems. *Toxicology letters* **161**, 108–114 (2006).
39. D, D. & L, D. Aldehyde oxidase and its role as a drug metabolizing enzyme. *Pharmacology & therapeutics* **201**, 137–180 (2019).
40. Wada, E. *et al.* Distribution of alpha2, alpha3, alpha4, and beta2 neuronal nicotinic receptor subunit mRNAs in the central nervous system: A hybridization histochemical study in the rat. *Journal of Comparative Neurology* **284**, 314–335 (1989).
41. Tribollet, E., Bertrand, D., Marguerat, A. & Raggenbass, M. Comparative distribution of nicotinic

receptor subtypes during development, adulthood and aging: An autoradiographic study in the rat brain. *Neuroscience* **124**, 405–420 (2004).
42. Buisson, B., Gopalakrishnan, M., Arneric, S. P., Sullivan, J. P. & Bertrand, D. Human α4β2 neuronal nicotinic acetylcholine receptor in HEK 293 cells: A patch-clamp study. *Journal of Neuroscience* **16**, 7880–7891 (1996).
43. Seguela, P., Wadiche, J., Dineley-Miller, K., Dani, J. A. & Patrick, J. W. Molecular cloning, functional properties, and distribution of rat brain α7: A nicotinic cation channel highly permeable to calcium. *Journal of Neuroscience* **13**, 596–604 (1993).
44. Williams, D. K., Wang, J. & Papke, R. L. Investigation of the molecular mechanism of the α7 nicotinic acetylcholine receptor positive allosteric modulator PNU-120596 provides evidence for two distinct desensitized states. *Molecular Pharmacology* **80**, 1013–1032 (2011).
45. Walsh, R. M. *et al.* Structural principles of distinct assemblies of the human α4β2 nicotinic receptor. *Nature* **557**, 261–265 (2018).
46. Ng, H. W. *et al.* Competitive docking model for prediction of the human nicotinic acetylcholine receptor α7 binding of tobacco constituents. *Oncotarget* **9**, 16899–16916 (2018).
47. Slotkin, T. A. If nicotine is a developmental neurotoxicant in animal studies, dare we recommend nicotine replacement therapy in pregnant women and adolescents? *Neurotoxicology and Teratology* vol. 30 1–19 (2008).
48. Azam, L., Chen, Y. & Leslie, F. M. Developmental regulation of nicotinic acetylcholine receptors within midbrain dopamine neurons. *Neuroscience* **144**, 1347–1360 (2007).
49. Xu, Z., Seidler, F. J., Ali, S. F., Slikker, J. & Slotkin, T. A. Fetal and adolescent nicotine administration: Effects on CNS serotonergic systems. *Brain Research* **914**, 166–178 (2001).
50. Slotkin, T. A., Cho, H. & Whitmore, W. L. Effects of prenatal nicotine exposure on neuronal development: Selective actions on central and peripheral catecholaminergic pathways. *Brain Research Bulletin* **18**, 601–611 (1987).
51. Smith, A. M., Dwoskin, L. P. & Pauly, J. R. Early exposure to nicotine during critical periods of brain development: Mechanisms and consequences. *Journal of Pediatric Biochemistry* **1**, 125–141 (2010).
52. Gillentine, M. A. *et al.* The Cognitive and Behavioral Phenotypes of Individuals with CHRNA7 Duplications. *Journal of Autism and Developmental Disorders* **47**, 549–562 (2017).
53. Ziats, M. N. *et al.* The complex behavioral phenotype of 15q13.3 microdeletion syndrome. *Genetics in Medicine* **18**, 1111–1118 (2016).
54. Deutsch, S. I., Burket, J. A., Benson, A. D. & Urbano, M. R. The 15q13.3 deletion syndrome: Deficient α7-containing nicotinic acetylcholine receptor-mediated neurotransmission in the pathogenesis of neurodevelopmental disorders. *Progress in Neuro-Psychopharmacology and Biological Psychiatry* vol. 64 109–117 (2016).
55. Marcus, M. M. *et al.* Alpha7 nicotinic acetylcholine receptor agonists and PAMs as adjunctive treatment in schizophrenia. An experimental study. *European Neuropsychopharmacology* **26**, 1401–1411 (2016).
56. Zhang, J.-C. *et al.* Depression-like phenotype by deletion of α7 nicotinic acetylcholine receptor: Role of BDNF-TrkB in nucleus accumbens OPEN. *Nature Publishing Group* (2016) doi:10.1038/srep36705.
57. Nacer, S. A. *et al.* Loss of α7 nicotinic acetylcholine receptors in GABAergic neurons causes sex-dependent decreases in radial glia-like cell quantity and impairments in cognitive and social behavior. *Brain Structure and Function* **226**, 365–379 (2021).
58. Felix, R. A. *et al.* Sensory Processing: Nicotinic acetylcholine receptor subunit α7-knockout mice exhibit degraded auditory temporal processing. *Journal of Neurophysiology* **122**, 451 (2019).
59. Levin, E. D. *et al.* Nicotinic α7- or β2-containing receptor knockout: Effects on radial-arm maze learning and long-term nicotine consumption in mice. *Behavioural Brain Research* **196**, 207–213 (2009).
60. Navarro, H. A. *et al.* Prenatal exposure to nicotine impairs nervous system development at a dose which does not affect viability or growth. *Brain Research Bulletin* **23**, 187–192 (1989).
61. Eppolito, A. K. & Smith, R. F. Long-term behavioral and developmental consequences of pre- and perinatal nicotine. *Pharmacology Biochemistry and Behavior* **85**, 835–841 (2006).
62. Nachmanoff, D. B. *et al.* Brainstem 3H-nicotine receptor binding in the sudden infant death syndrome. *Journal of neuropathology and experimental neurology* **57**, 1018–1025 (1998).
63. Slotkin, T. A., Pinkerton, K. E., Auman, J. T., Qiao, D. & Seidler, F. J. Perinatal exposure to

environmental tobacco smoke upregulates nicotinic cholinergic receptors in monkey brain. *Developmental Brain Research* **133**, 175–179 (2002).
64. Frazier, C. J. *et al. Acetylcholine Activates an-Bungarotoxin-Sensitive Nicotinic Current in Rat Hippocampal Interneurons, But Not Pyramidal Cells*. (1998).
65. Cheng, Q. & Yakel, J. L. The effect of α7 nicotinic receptor activation on glutamatergic transmission in the hippocampus. *Biochemical Pharmacology* vol. 97 439–444 (2015).
66. Slotkin, T. A., Ryde, I. T., Tate, C. A. & Seidler, F. J. Lasting effects of nicotine treatment and withdrawal on serotonergic systems and cell signaling in rat brain regions: Separate or sequential exposure during fetal development and adulthood. *Brain Research Bulletin* **73**, 259–272 (2007).
67. Slotkin, T. A., Tate, C. A., Cousins, M. M. & Seidler, F. J. Prenatal nicotine exposure alters the responses to subsequent nicotine administration and withdrawal in adolescence: Serotonin receptors and cell signaling. *Neuropsychopharmacology* **31**, 2462–2475 (2006).
68. Sachana, M., Rolaki, A. & Bal-Price, A. Development of the Adverse Outcome Pathway (AOP): Chronic binding of antagonist to N-methyl-D-aspartate receptors (NMDARs) during brain development induces impairment of learning and memory abilities of children. *Toxicology and Applied Pharmacology* **354**, (2018).
69. Noviello, C. M. *et al.* Structure and gating mechanism of the α7 nicotinic acetylcholine receptor. *Cell* **184**, 2121-2134.e13 (2021).
70. W, S., T, D., MP, J., RA, F. & R, F. Novel procedure for modeling ligand/receptor induced fit effects. *Journal of medicinal chemistry* **49**, 534–553 (2006).
71. Ihara, M. *et al.* Crystal structures of Lymnaea stagnalis AChBP in complex with neonicotinoid insecticides imidacloprid and clothianidin. *Invertebrate Neuroscience* **8**, 71–81 (2008).
72. Scholz, D. *et al.* Rapid, complete and large-scale generation of post-mitotic neurons from the human LUHMES cell line. *Journal of Neurochemistry* **119**, 957–971 (2011).
73. Stiegler, N. V., Krug, A. K., Matt, F. & Leist, M. Assessment of chemical-induced impairment of human neurite outgrowth by multiparametric live cell imaging in high-density cultures. *Toxicological Sciences* **121**, 73–87 (2011).
74. Krug, A. K. *et al.* Evaluation of a human neurite growth assay as specific screen for developmental neurotoxicants. *Arch Toxicol* **3**, 2215–2231 (2013).
75. Mica, Y., Lee, G., Chambers, S. M., Tomishima, M. J. & Studer, L. Modeling Neural Crest Induction, Melanocyte Specification, and Disease-Related Pigmentation Defects in hESCs and Patient-Specific iPSCs. *Cell Reports* **3**, 1140–1152 (2013).
76. Chambers, S. M. *et al.* Highly efficient neural conversion of human ES and iPS cells by dual inhibition of SMAD signaling. *Nature Biotechnology* **27**, 275–280 (2009).
77. Dreser, N. *et al.* Development of a neural rosette formation assay (RoFA) to identify neurodevelopmental toxicants and to characterize their transcriptome disturbances. *Archives of Toxicology* **94**, 151–171 (2020).
78. Baud, A. *et al.* Multiplex High-Throughput Targeted Proteomic Assay to Identify Induced Pluripotent Stem Cells. *Analytical Chemistry* **89**, 2440–2448 (2017).
79. Hoelting, L. *et al.* Stem Cell-Derived Immature Human Dorsal Root Ganglia Neurons to Identify Peripheral Neurotoxicants. *STEM CELLS Translational Medicine* **5**, 476–487 (2016).
80. *Test No. 236: Fish Embryo Acute Toxicity (FET) Test*. (OECD, 2013). doi:10.1787/9789264203709-en.
81. von Hellfeld, R., Brotzmann, K., Baumann, L., Strecker, R. & Braunbeck, T. Adverse effects in the fish embryo acute toxicity (FET) test: a catalogue of unspecific morphological changes versus more specific effects in zebrafish (Danio rerio) embryos. *Environmental Sciences Europe* **32**, 122 (2020).
82. Zindler, F. *et al.* Analysis of tail coiling activity of zebrafish (Danio rerio) embryos allows for the differentiation of neurotoxicants with different modes of action. *Ecotoxicology and Environmental Safety* **186**, (2019).
83. Burg, B. van der *et al.* A Panel of Quantitative Calux® Reporter Gene Assays for Reliable High-Throughput Toxicity Screening of Chemicals and Complex Mixtures. *High-Throughput Screening Methods in Toxicity Testing* 519–532 (2013) doi:10.1002/9781118538203.CH28.
84. House, J. S. *et al.* A Pipeline for High-Throughput Concentration Response Modeling of Gene Expression for Toxicogenomics. *Frontiers in Genetics* **8**, 168 (2017).
85. O'Brien, J., Wilson, I., Orton, T. & Pognan, F. Investigation of the Alamar Blue (resazurin) fluorescent dye for the assessment of mammalian cell cytotoxicity. *European Journal of Biochemistry* **267**, 5421–5426 (2000).

86. Delp, J. *et al.* A high-throughput approach to identify specific neurotoxicants/ developmental toxicants in human neuronal cell function assays. *ALTEX* **35**, 235–253 (2018).
87. Nyffeler, J. *et al.* Design of a high-Throughput human neural crest cell migration assay to indicate potential developmental toxicants. *Altex* **34**, 75–94 (2017).
88. Ihara, M. *et al.* Studies on an acetylcholine binding protein identify a basic residue in loop G on the β1 strand as a new structural determinant of neonicotinoid actions. *Molecular Pharmacology* **86**, 736–746 (2014).
89. Rodgers, T. & Rowland, M. Physiologically based pharmacokinetic modelling 2: Predicting the tissue distribution of acids, very weak bases, neutrals and zwitterions. *Journal of Pharmaceutical Sciences* **95**, 1238–1257 (2006).
90. K, S. Theoretical investigation of passive intestinal membrane permeability using Monte Carlo method to generate drug-like molecule population. *International journal of pharmaceutics* **373**, 55–61 (2009).
91. Jamei, M. *et al.* The Simcyp® population-based ADME simulator. *Expert Opinion on Drug Metabolism and Toxicology* vol. 5 211–223 (2009).
92. Harada, K. H. *et al.* Biological Monitoring of human exposure to neonicotinoids using urine samples, and neonicotinoid excretion kinetics. *PLoS ONE* **11**, e0146335 (2016).
93. CL, M.-P., CM, N. & RE, H. X-ray structure of the human α4β2 nicotinic receptor. *Nature* **538**, 411–415 (2016).
94. DA, D. The cation-π interaction. *Accounts of chemical research* **46**, 885–893 (2013).
95. M, T. *et al.* Atypical nicotinic agonist bound conformations conferring subtype selectivity. *Proceedings of the National Academy of Sciences of the United States of America* **105**, 1728–1732 (2008).
96. Bailey, J., Oliveri, A. & Levin, E. D. Zebrafish model systems for developmental neurobehavioral toxicology. *Birth Defects Research Part C: Embryo Today: Reviews* **99**, 14–23 (2013).
97. De Esch, C., Slieker, R., Wolterbeek, A., Woutersen, R. & de Groot, D. Zebrafish as potential model for developmental neurotoxicity testing: A mini review. *Neurotoxicology and Teratology* **34**, 545–553 (2012).
98. Nishimura, Y. *et al.* Zebrafish as a systems toxicology model for developmental neurotoxicity testing. *Congenital Anomalies* **55**, 1–16 (2015).
99. Tierney, K. B. Behavioural assessments of neurotoxic effects and neurodegeneration in zebrafish. *Biochimica et Biophysica Acta (BBA) - Molecular Basis of Disease* **1812**, 381–389 (2011).
100. Xu, X., Scott-Scheiern, T., Kempker, L. & Simons, K. Active avoidance conditioning in zebrafish (Danio rerio). *Neurobiology of Learning and Memory* **87**, 72–77 (2007).
101. Saint-Amant, L. & Drapeau, P. Time Course of the Development of Motor Behaviors in the Zebrafish Embryo. *J Neurobiol* **37**, 622–632 (1998).
102. Saint-Amant, L. & Drapeau, P. Motoneuron Activity Patterns Related to the Earliest Behavior of the Zebrafish Embryo. *Journal of Neuroscience* **20**, 3964–3972 (2000).
103. Zindler, F., Beedgen, F. & Braunbeck, T. Time-course of coiling activity in zebrafish (Danio rerio) embryos exposed to ethanol as an endpoint for developmental neurotoxicity (DNT) – Hidden potential and underestimated challenges. *Chemosphere* **235**, 12–20 (2019).
104. Zindler, F. *et al.* Do environmentally relevant concentrations of fluoxetine and citalopram impair stress-related behavior in zebrafish (Danio rerio) embryos? *Chemosphere* **261**, 127753 (2020).
105. Selderslaghs, I. W. T., Hooyberghs, J., De Coen, W. & Witters, H. E. Locomotor activity in zebrafish embryos: A new method to assess developmental neurotoxicity. *Neurotoxicology and Teratology* **32**, 460–471 (2010).
106. IW, S., J, H., R, B. & HE, W. Assessment of the developmental neurotoxicity of compounds by measuring locomotor activity in zebrafish embryos and larvae. *Neurotoxicology and teratology* **37**, 44–56 (2013).
107. Weichert, F. G., Floeter, C., Meza Artmann, A. S. & Kammann, U. Assessing the ecotoxicity of potentially neurotoxic substances – Evaluation of a behavioural parameter in the embryogenesis of Danio rerio. *Chemosphere* **186**, 43–50 (2017).
108. Velki, M., Di Paolo, C., Nelles, J., Seiler, T. B. & Hollert, H. Diuron and diazinon alter the behavior of zebrafish embryos and larvae in the absence of acute toxicity. *Chemosphere* **180**, 65–76 (2017).
109. Draft Assessment Report (DAR)-public version-Initial risk assessment provided by the rapporteur Member State Germany for the existing active substance.
110. JL, B., M, M., J, F. & LP, B. Human intestinal absorption of imidacloprid with Caco-2 cells as

enterocyte model. *Toxicology and applied pharmacology* **194**, 1–9 (2004).
111. E.Lammera, G.J.Carrb, K.Wendlera, J.M.Rawlingsb, S.E.Belangerb, Th.Braunbecka (2008), Is the fish embryo toxicity test (FET) with the zebrafish (Danio rerio) a potential alternative for the fish acute toxicity test?, Comparative Biochemistry and Physiology Part C: Toxicology & Pharmacology Volume 149, Issue 2, March 2009, Pages 196-209
112. Thomas Braunbeck, Britta Kais, Eva Lammer, Jens Otte, Katharina Schneider, Daniel Stengel & Ruben Strecker (2015). The fish embryo test (FET): origin, applications, and future, Environmental Science and Pollution Research volume 22, pages16247–16261 (2015)

Annex I: ZFE method

Figure 31 (ZFEX1). Methods of the FET test, coiling assay and basal swimming assay, conducted with the zebrafish (Danio rerio) embryo.

The following method descriptions and statistical analysis protocols can be found in von Hellfeld et al., (unpublished).

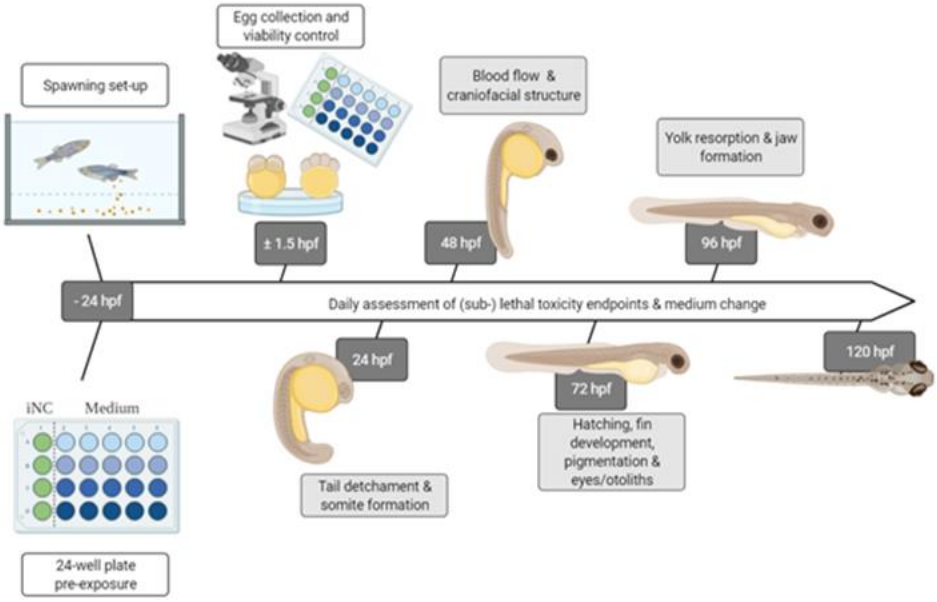

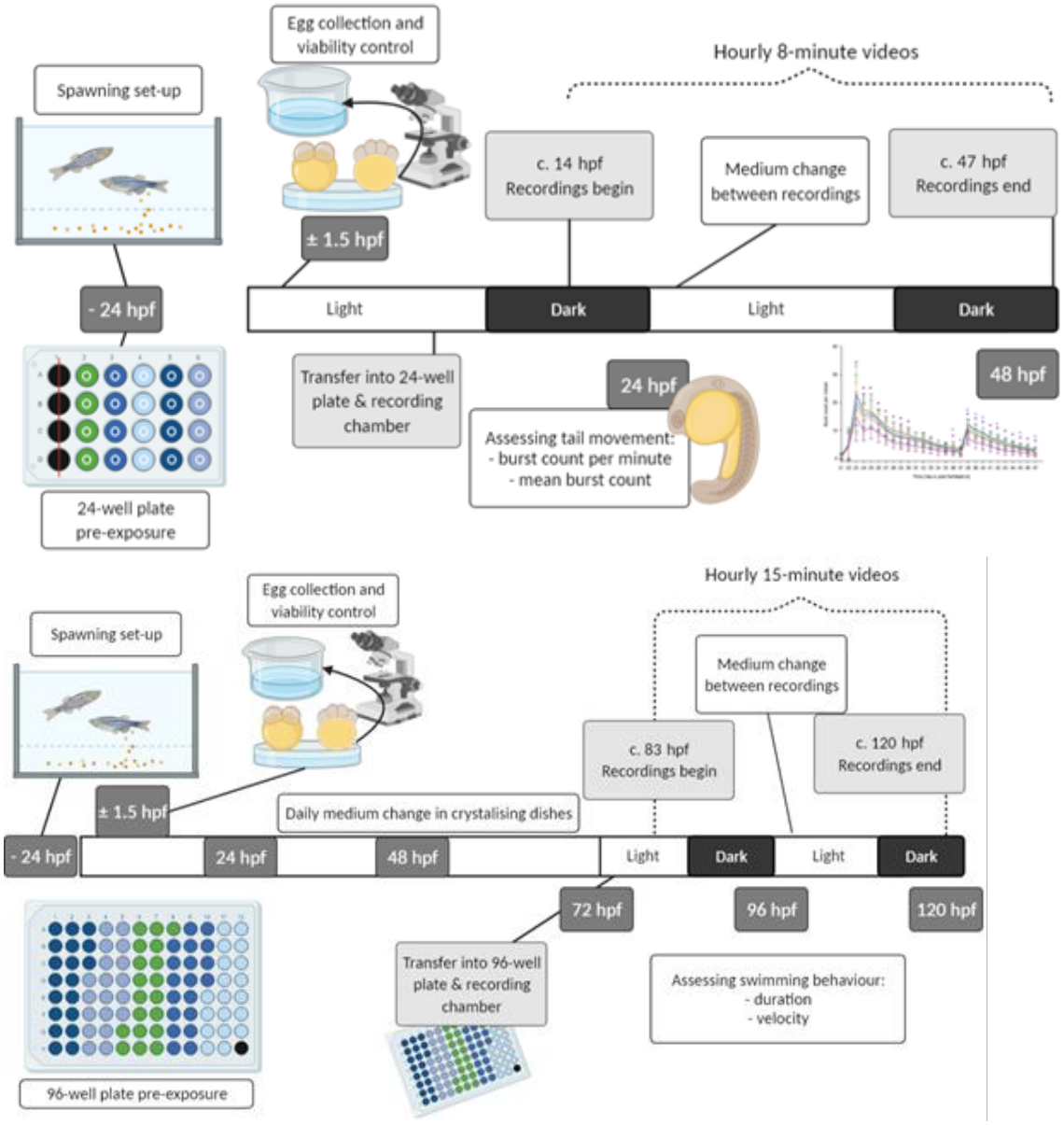

Zebrafish handling and maintenance: Adult 'Westaquarium' strain zebrafish are kept and reared in the breeding facilities at the Aquatic Ecology and Toxicology Group (Centre for Organismal Studies; University of Heidelberg; Heidelberg; Germany; license no. 35-9185.64/BH). In accordance with the OECD TG 236, the maintenance, breeding conditions and egg production was conducted based on internationally accepted standards (Lammer et al., 2009). For all assays, the OECD TG 236 standardized water was prepared freshly in-house and the egg collection and handling process of the guideline was followed (OECD, 2013): Freshly laid eggs (<1 hpf) were transferred to 50 ml crystallizing dishes filled with the respective test solutions. For the behavioral assays, the embryos were reared in crystallizing dishes. Total medium renewal was done daily (semi-static exposure) and where recordings were part of the protocol, renewal was conducted between recordings, replacing the well plate at least 20 minutes prior to the next recording for re-acclimatization.

Coiling assay: For each biological replicate (n=3), five 7 hpf embryos were transferred into each well of a 24-well plate (TPP, Trasadingen, Switzerland) containing 2 ml fresh test solution (n=20 technical replicates per biological replicate). The well plates had previously been pre-exposed to the respective concentration medium to account for compound adsorption to the plastic. The embryos were centered with a 5.3 mm diameter polytetrafluoroethylene ring (ESSKA, Hamburg, Germany). The concentration order in the 24-well plate was randomized, containing four test concentrations, as well as a solvent control (0.1% DMSO) utilized here as the "untreated control group". The plate was placed on an acrylic glass covered light box (twelve infrared lights, 880 nm 40° 5 mm, Knightbright, Taiwan) in an incubator (HettCube 600R, Hettich, Tuttlingen,Germany) at 26 ± 1 °C set to a 14/10 h light/dark cycle. The incubator further contained a large water reservoir to prevent medium evaporation from the un-covered well plate. 8-minute long (mpeg-4, 25 frames/s) videos were filmed between 21 and 47 hpf (Camera: Basler acA1920-155µm, Ahrensburg, Germany; Lens: M7528-MP F2.8 f75mm, Computar®, Basler, Ahrensburg, Germany; Germany; Filter: heliopan, RG850, Gräfelfing, Germany) utilizing the Ethovision® Software (Noldus, Wageningen, Netherlands). To avoid unnecessary movement of the recording set-up through the vibrations of the capacitor, the incubator was switched off for 15 minutes every hour, 3 minutes prior to the onset of recording (as outlined by Zindler et al., 2019). The lights were not affected by the hourly incubator switch-off. Details of parameter settings can be found in Table 9 below.

Basal swimming assay: At 72 hpf, 1 embryo per well was transferred into 96-well plates (TPP, Trasadingen, Switzerland), containing 360 µl fresh test solution per well (n=19 technical replicates per biological replicate (n=3) for nicotine, and n=2 biological replicates for acetamiprid). The well plates had previously been pre-exposed to the respective concentration medium to account for compound adsorption. The plate was then placed in the DanioVision Observation Chamber (Noldus, Wageningen, Netherlands) and thermostatically controlled through flow (DanioVision external Temperature Control Unit) ensured a constant water temperature of 26 ± 1 °C and a 14/10 h light/dark cycle. 15-Minute videos were recorded every hour between 83 and 120 hpf, using EthoVision Software (Noldus, Wageningen, Netherlands) (Zindler, Beedgen, Brandt, et al., 2019). The videos were then analyzed with Danioscope® Software (Version 1.1). Details of parameter settings can be found in Table 9 below.

Table 9 ZFEX1. Parameter-settings in the EthioVision(R)TX software for video recordings, as well as camera settings.

The table was adapted from von Hellfeld et al., (unpublished)

	Setting	Parameter
Coil	**Video settings**	
	Basler acA1920-155um	1600x1200
	Gain Auto	Off
	Gain Selector	All
	Gain	1,00000
	Black Level Selector	All
	Black Level	0,00000
	Gamma	1,00000
	Digital shift	4
	Detection settings	
	Activity onset	2%
	Activity offset	0.5%
	Minimum inter peak interval	100 ms
	Minimum peak duration	0 ms
Swim	**Video settings**	
	Basler acA1300-60gm	1280x960
	Gain Auto	Off
	Gain Selector	Analog All

	Gain (Raw)	0
	Black Level Selector	All
	Black Level (Raw)	50
	Gamma Enable	Disabled
	Gamma Selector	User
	Gamma	1
	Digital Shift	1
	Detection Settings	
	Method	DanioVision
	Detection Sensitivity	160
	Activity Threshold	100
	Activity Background noise filter	5
	Compression artifacts filter	On

Statistical analysis: For all assays, the biological replicates were initially evaluated individually and compared to the respective controls. ToxRat® (version 2.10.03; ToxRat™ Solutions, Alsdorf, Germany), GraphPad Prism version 7.03 for Windows (GraphPad, La Jolla, California, USA), and the open-source statistical software RStudio (Version 1.3.959) interface running R software (Version 4.0.2 for Windows; R Developmental Core Team, 2020), were used for statistical computing and SigmaPlot Version 14.0 (Systat Software Inc., San Jose, California, USA) for visual data representation. Additionally, the free software Inkscape (Software 0.92.4, 5da689c313, 2019-01-14) was used for post-editing of vector graphs. Differences are declared to be statistically significant at $p < 0.05$.

FET test: Effect concentrations (EC) were calculated at effect levels of 10 and 50% based on probit analysis using linear maximum likelihood regression with ToxRat® (Braunbeck *et al*., 2015). Due to the overall low frequency of observed sub-lethal effects, however, all three replicates were assessed simultaneously with ToxRat®.

Coiling assay: The videos were analyzed with the Danioscope Software (Version 1.1) and the read-out data for mean burst duration [seconds] and burst count per minute were obtained as excel spread sheets. ANOVA on ranks (Kruskal Wallis test) was utilized to analyze the differences in means of the behavior parameters compared to the untreated control group, followed by the Dunn's *post hoc* test against controls; carried out separately for each replicate, using GraphPad Prism. Time points at which at least two of three replicates were found to be statistically significant ($p \leq 0.05$) were considered as an effect caused by the exposure.

Basal swimming assay: Swimming distance in the basal swimming assay was evaluated by summarizing the data into bins of 3 to 5 hours. Outlier screening was conducted with the R function 'identify_outliers' (rstatix package, Version 0.5.0) for each biological replicate. The distance moved parameter was handled as follows: 1) the raw data was examined, and estimates scored >1.0% (the cut-off threshold) in 'missed samples' were removed and the remaining data pooled into 3-5 h bins. An outlier check with R was implemented, followed by non-parametric analysis and the Dunn's *post hoc* test. 2) The total distance moved over the recorded 25 h was estimated by summing up the distance moved per individual over all time points. This data was assessed parametric one-way analysis of variance (ANOVA), and multiple comparisons of means from treatment groups against a control group (Dunnett's test, package 'multcomp', Version 1.4.13). Effect size was estimated in terms of eta-squared (η^2) and can be interpreted as follows: 0-0.010: no effect, 0.010-0.060: small effect, 0.060-0.140: intermediate effect, and 0.140-0.200: large effect. To determine swimming frequency, raw data was assessed in time steps of 0.4 s and considered as a movement in events where activity was registered after a period of at least 5 seconds without movement, allowing to distinguish between actual movement and background noise.

Table 10 ZFEX2. p-values of the coiling assay Kruskal-Wallis and Dunns post hoc test.
At least 2 biological replicates must have indicated a significant difference between the control group and a treatment group to classify as significant. Nicotine (NIC) was tested in 3 biological replicates, whilst acetamiprid (ACE) was tested in 4 biological replicates until 37 hpf, and in 1 biological replicate until 47 hpf. Where only one value is noted, this p-value threshold was observed in both biological replicates. Table adapted from von Hellfeld et al., (unpublished)

	Mean burst duration			Mean burst count per minute		
	Conc. [µM]	hpf	*p*-value(s)	Conc. [µM]	hpf	*p*-value(s)
NIC	1.25	39, 40	≤0.001, ≤0.01, ≤0.05	1.25	30, 34	≤0.01, ≤0.05
		41–45	≤0.001, ≤0.01		36	≤0.01
	2.5	23	≤0.001, ≤0.01		37, 38, 40-42, 47	≤0.001
		24	≤0.001, ≤0.05		39, 43, 46	≤0.001, ≤0.05
		28, 38, 39, 41, 46	≤0.01, ≤0.05		44, 45	≤0.001, ≤0.01
		40, 45	≤0.01	2.5	23, 25, 40-47	≤0.001
		42-44	≤0.001, ≤0.01, ≤0.05		24, 38, 39	≤0.001, ≤0.01
	12.5	23, 30, 38, 45, 46	≤0.001, ≤0.01		33	≤0.01, ≤0.05
		24-29, 31, 39-44, 47	≤0.001		35	≤0.05
	25	23-47	≤0.001		37	≤0.001, ≤0.01, ≤0.05
				12.5	23-26	≤0.001
					27, 34, 45-47	≤0.001, ≤0.01
					33	≤0.01
					35, 44	≤0.001, ≤0.05
					36	≤0.001, ≤0.01, ≤0.05
					37	≤0.05
				25	23, 40	≤0.001, ≤0.05
					24-28	≤0.001
					29-33	≤0.001, ≤0.01
					34	≤0.001, ≤0.01, ≤0.05
					40-42	≤0.01, ≤0.05
					43, 44	≤0.05
ACE*	25	31	≤0.05	2.5	23	≤0.001
		39	≤0.05	25	23	≤0.001
		40	≤0.001		24	≤0.01, ≤0.001
	50	40 - 42	≤0.05		33	≤0.05
		44	≤0.01		38, 39, 43, 45	≤0.05

	100	38	≤0.001		40, 42	≤0.01
		39 - 41	≤0.001		44, 46	0.001
		42, 44	≤0.01	50	23	≤0.01, ≤0.001
		45	≤0.05		24	≤0.001
					42, 45	≤0.05
					44, 46	≤0.001
				100	23	≤0.001, ≤0.05
					24	≤0.001, ≤0.01, ≤0.05
					25	≤0.01
					33, 34	≤0.001, ≤0,05
					44	≤0.01

Blue box: The respective value is based on one biological replicate (n=20 technical replicates)

Table 11 ZFEX3. p-values of the basal swimming assay Kruskal-Wallis and Dunns post hoc test (n=2).

Where only one value is noted, this p-value threshold was observed in both biological replicates. Table adapted from von Hellfeld et al., (unpublished)

Distance moved [mm]			Mean burst count per minute		
Concentration	hpf	*p*-value(s)	Concentration	hpf	*p*-value(s)
100 µM	100-104	=0.01, =0.05	100 µM	110-114	=0.05
	110-114	=0.001, =0.05			

ANNEX II: PBPK report

Please refer to the separate publication for full Annex I.
ENV/CBC/MONO(2022)27/ANN1.